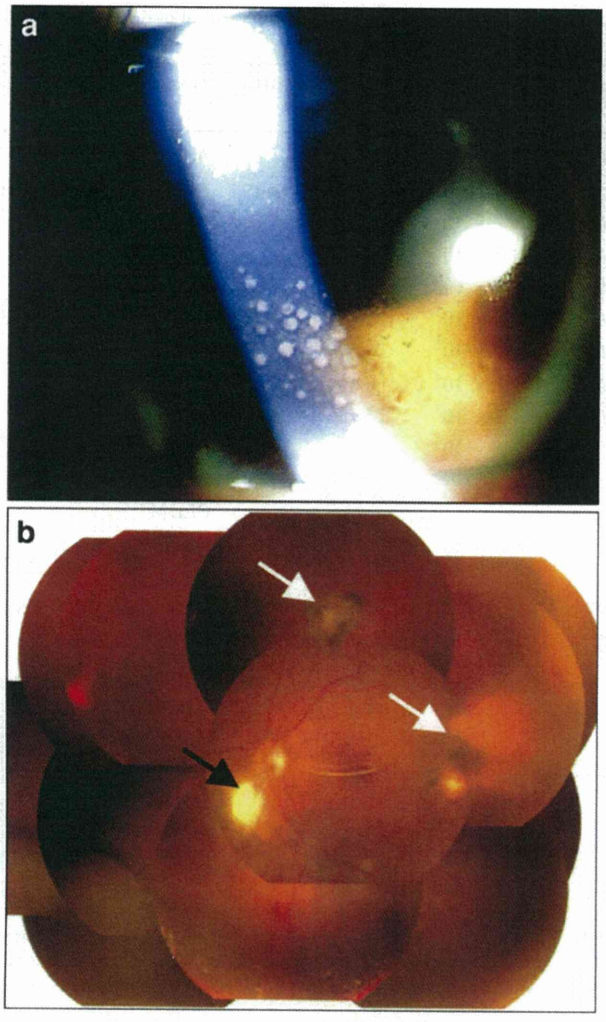

Fig. 2 Fundus and slit photograph of a patient with ocular toxoplasmosis (Case 1 in Table 3). **a** Slit and fundus photograph. **b** OS of a patient with an active toxoplasmosis infection. Diffuse keratic precipitates and anterior chamber cells (*upper panel*), and retinal yellowish white mass lesions (Edmund–Jensen type: *black arrow*) and retinal-pigmented exudates (*white arrows*) together with vitreous opacities are seen (*lower panel*)

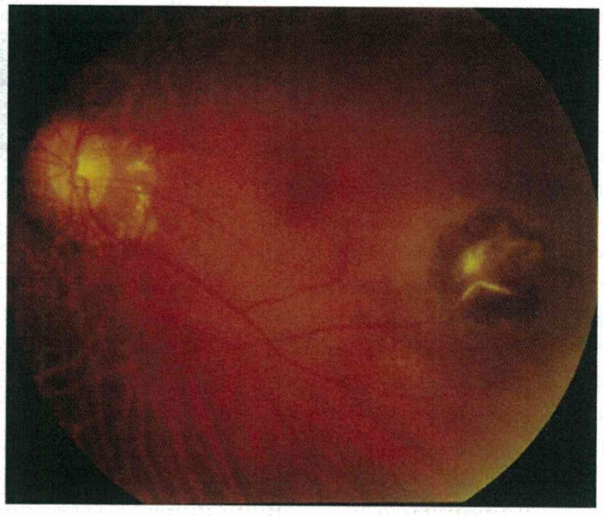

Fig. 3 A fundus photograph OS from an inactive ocular toxoplasmosis patient (Case 11 in Table 3). Old pigmented retinal exudates without inflammatory signs (vitreous cells, vitreous opacity, or retinal vasculitis) can be seen. PCR assay results were negative for genomic DNA of *T. gondii*

the proposed PCR system may be more advantageous since it has the ability to quantify the infection load of a clinical specimen. In addition, PCR examinations can exclude other major ocular infections that are caused by the human herpes virus. Westeneng et al. [7] reported 10 cases of ocular toxoplasmosis in immunocompromised patients. The PCR results were initially negative in 6 of these patients, with diagnosis only confirmed after use of the GWC. On the other hand, de Boer et al. report the use of PCR analysis was preferred for immunocompromised patients, because production of the local specific antibodies can be unpredictable in such patients [10]. Although the use of either PCR or GWC to diagnose ocular toxoplasmosis remains controversial, we were able to use PCR to detect the genomic DNA of toxoplasmosis in our immunocompetent patients even when they only had an active ocular inflammation. Therefore, this PCR methodology may be useful for *T. gondii* infection screening when used in conjunction with other diagnostic techniques, for example routine serological tests. In this study, we found increased anti-toxoplasma IgG in the serum of all of the ocular toxoplasmosis patients. However, we also found increased anti-toxoplasma IgG in the serum of two of our uveitis patients without ocular toxoplasmosis (Cases 14 and 22 in Table 3). We therefore recommend that PCR also be used to measure the toxoplasma DNA in ocular samples.

The protozoan parasite *T. gondii* has emerged as an important opportunistic infectious pathogen. In the eye, *T. gondii* infections can cause granulomatous pan-uveitis and necrotic retinitis, with typical ocular inflammation indicative of focal retinal necrosis, vitreous opacity, anterior chamber cells, and choroidal edema. Fundus lesions seen in ocular toxoplasmosis can be atypical in many patients, resembling necrotizing retinitis caused by human herpes viruses. The new PCR method is particularly useful when screening those uveitis patients who usually fail to generate specific IgM or increased IgG titers for *T. gondii* or who have had focal retinal necrosis. Thus, these results can be used to distinguish the findings from other retinal necrotic disorders, for example acute retinal necrosis and cytomegalovirus retinitis. By using several different primer pairs in LightCycler capillaries, these methods proved capable of rapidly screening for detection of the genome of

all eight types of human herpes virus and *T. gondii*. Development of this multiplex and real-time PCR assay seems to be quite advantageous, because this methodology makes it possible to exclude non-toxoplasma uveitis patients.

In conclusion, we have established a rapid, sensitive, comprehensive, two-step PCR system that can be used to detect *T. gondii*. New studies that examine larger numbers of samples from suspected ocular toxoplasmosis patients will need to be undertaken in the future in order to definitively establish the clinical value of this new diagnostic technique.

Acknowledgments Drs Kazuichi Maruyama and Kenji Nagata of the Department of Ophthalmology, Kyoto Prefectural University of Medicine, collected and sent the samples used in this study. We are grateful for the expert technical assistance of Mr Ken Watanabe. This work was supported by Comprehensive Research on Disability, Health and Welfare, Health and Labour Sciences Research Grants, Ministry Health, Labour and Welfare, Japan.

References

1. Aouizerate F, Cazenave J, Poirier L, Verin P, Cheyrou A, Begueret J, et al. Detection of *Toxoplasma gondii* in aqueous humour by the polymerase chain reaction. Br J Ophthalmol. 1993;77:107–9.
2. Manners RM, O'Connell S, Guy EC, Joynson DH, Canning CR, Etchells DE. Use of the polymerase chain reaction in the diagnosis of acquired ocular toxoplasmosis in an immunocompetent adult. Br J Ophthalmol. 1994;78:583–4.
3. Robert-Gangneux F, Binisti P, Antonetti D, Brezin A, Yera H, Dupouy-Camet J. Usefulness of immunoblotting and Goldmann–Witmer coefficient for biological diagnosis of toxoplasmic retinochoroiditis. Eur J Clin Microbiol Infect Dis. 2004;23:34–8.
4. De Groot-Mijnes JD, Rothova A, Van Loon AM, Martinus RA, Völker R, ten Dam-van Loon NH, et al. Polymerase chain reaction and Goldmann–Witmer coefficient analysis are complimentary for the diagnosis of infectious uveitis. Am J Ophthalmol. 2006;141:313–8.
5. Kijlstra A, Luyendijk L, Baarsma GS, Rothova A, Schweitzer CM, Timmerman Z, et al. Aqueous humor analysis as a diagnostic tool in toxoplasma uveitis. Int Ophthalmol. 1989;13:383–6.
6. Witmer R. Clinical implications of aqueous humor studies in uveitis. Am J Ophthalmol. 1978;86:39–44.
7. Westeneng AC, Rothova A, de Boer JH, de Groot-Mijnes JD. Infectious uveitis in immunocompromised patients and the diagnostic value of polymerase chain reaction and Goldmann–Witmer coefficient in aqueous analysis. Am J Ophthalmol. 2007;144:781–5.
8. Matos K, Muccioli C, Belfort Junior R, Rizzo LV. Correlation between clinical diagnosis and PCR analysis of serum, aqueous, and vitreous samples in patients with inflammatory eye disease. Arq Bras Oftalmol. 2007;70:109–14.
9. Rothova A, de Boer JH, Ten Dam-van Loon NH, Postma G, de Visser L, Zuurveen SJ, et al. Usefulness of aqueous humor analysis for the diagnosis of posterior uveitis. Ophthalmology. 2008;115:306–11.
10. de Boer JH, Verhagen C, Bruinenberg M, Rothova A, de Jong PT, Baarsma GS, et al. Serologic and polymerase chain reaction analysis of intraocular fluids in the diagnosis of infectious uveitis. Am J Ophthalmol. 1996;121:650–8.
11. Figueroa MS, Bou G, Marti-Belda P, Lopez-Velez R, Guerrero A. Diagnostic value of polymerase chain reaction in blood and aqueous humor in immunocompetent patients with ocular toxoplasmosis. Retina. 2000;20:614–9.
12. Bottós J, Miller RH, Belfort RN, Macedo AC, UNIFESP Toxoplasmosis Group, Belfort R Jr, et al. Bilateral retinochoroiditis caused by an atypical strain of *Toxoplasma gondii*. Br J Ophthalmol. 2009;93:1546–50.
13. Lin MH, Chen TC, Kuo TT, Tseng CC, Tseng CP. Real-time PCR for quantitative detection of *Toxoplasma gondii*. J Clin Microbiol. 2000;38:4121–5.
14. Patrat-Delon S, Gangneux JP, Lavoué S, Lelong B, Guiguen C, le Tulzo Y, et al. Correlation of parasite load determined by quantitative PCR to clinical outcome in a heart transplant patient with disseminated toxoplasmosis. J Clin Microbiol. 2010;48:2541–5.
15. Fekkar A, Bodaghi B, Touafek F, Le Hoang P, Mazier D, Paris L. Comparison of immunoblotting, calculation of the Goldmann–Witmer coefficient, and real-time PCR using aqueous humor samples for diagnosis of ocular toxoplasmosis. J Clin Microbiol. 2008;46:1965–7.
16. Cassaing S, Bessières MH, Berry A, Berrebi A, Fabre R, Magnaval JF. Comparison between two amplification sets for molecular diagnosis of toxoplasmosis by real-time PCR. J Clin Microbiol. 2006;44:720–4.
17. Sugita S, Shimizu N, Watanabe K, Mizukami M, Morio T, Sugamoto Y, et al. Use of multiplex PCR and real-time PCR to detect human herpes virus genome in ocular fluids of patients with uveitis. Br J Ophthalmol. 2008;92:928–32.
18. Sugita S, Iwanaga Y, Kawaguchi T, Futagami Y, Horie S, Usui T, et al. Detection of herpesvirus genome by multiplex polymerase chain reaction (PCR) and real-time PCR in ocular fluids of patients with acute retinal necrosis. Nippon Ganka Gakkai Zasshi. 2008;112:30–8.
19. Sugita S, Shimizu N, Watanabe K, Katayama M, Horie S, Ogawa M, et al. Diagnosis of bacterial endophthalmitis by broad-range quantitative polymerase chain reaction. Br J Ophthalmol. 2011;95:345–9.

Graefes Arch Clin Exp Ophthalmol
DOI 10.1007/s00417-011-1819-1

INFLAMMATORY DISORDERS

Detection of *Candida* and *Aspergillus* species DNA using broad-range real-time PCR for fungal endophthalmitis

Sunao Sugita · Koju Kamoi · Manabu Ogawa · Ken Watanabe · Norio Shimizu · Manabu Mochizuki

Received: 24 June 2011 / Revised: 29 August 2011 / Accepted: 2 September 2011

Abstract
Background The goal of this work is to establish a broad-range real-time polymerase chain reaction (PCR) diagnostic system for ocular fungal infection and to measure *Candida* and *Aspergillus* DNA in the ocular fluids obtained from unknown uveitis/endophthalmitis patients.
Methods After obtaining informed consent, intraocular fluids (aqueous humor and vitreous fluid samples) were collected from 54 patients with idiopathic uveitis or endophthalmitis. Samples were assayed for *Candida* or *Aspergillus* DNA using broad-range (18S rRNA sequences) quantitative real-time PCR.
Results *Candida* or *Aspergillus* DNA was detected in seven out of 54 patient ocular samples (13%). These PCR-positive samples showed significantly high copy numbers of *Candida* or *Aspergillus* DNA. On the other hand, fungal DNA was not detected in any of the other 46 samples collected from these idiopathic uveitis or endophthalmitis patients. In the one PCR-negative case, PCR did not detect any fungal genome in the sample, even though this patient was clinically suspected of having *Candida* endophthalmitis. Real-time PCR results were negative for fungal DNA in the bacterial endophthalmitis patients and in various uveitis patients. In addition, fungal DNA was also not detected in patients without ocular inflammation (controls).
Conclusions Analysis of ocular samples by this broad-range real-time PCR method can be utilized for rapid diagnosis of patients suffering from unknown intraocular disorders such as idiopathic uveitis/endophthalmitis.

Keywords Endophthalmitis · Fungal infection · Polymerase chain reaction

S. Sugita (✉) · K. Kamoi · M. Ogawa · M. Mochizuki
Department of Ophthalmology & Visual Science,
Tokyo Medical and Dental University,
Graduate School of Medical and Dental Sciences,
1-5-45 Yushima,
Bunkyo-ku, Tokyo 113-8519, Japan
e-mail: sunaoph@tmd.ac.jp

K. Watanabe · N. Shimizu
Department of Virology, Division of Medical Science,
Tokyo Medical and Dental University,
Graduate School of Medical and Dental Sciences,
Tokyo, Japan

Introduction

Fungal endophthalmitis is a sight-threatening disease caused by human pathogenic fungi. Fungal infections are known to cause ocular inflammations such as endophthalmitis, uveitis, and keratitis. However, with the exception of for the *Candida*-associated ocular infection, the association between the fungus and the observed clinical features has yet to be elucidated. The well-known clinical features for *Candida* endophthalmitis include a fungal ball in the retina and vitreous opacity [1]. Fungal endophthalmitis can result from hematogenous dissemination or from a direct inoculation following trauma or surgery to the eye. Risk factors for fungal endophthalmitis include intravascular catheters, diabetes, malignancy, chemotherapeutic agents, and steroids. However, the clinical findings can be very diverse in some cases of ocular inflammatory disorders caused by fungal species. Moreover, fungal infections have been widely associated with keratitis, retinitis, uveitis, retinal/choroidal vasculitis, invasive orbital infection, and endophthalmitis. Because of this diversity, infection diagnosis is both difficult and time-consuming [1–4]. In order to be able to perform adequate treatments that can prevent these infectious agents from causing irreversible ocular damage,

Published online: 27 September 2011

early examinations that correctly identify the etiology of the infection are necessary.

Conventional methods of diagnosis of fungal endophthalmitis include detection and isolation of the fungi from the intraocular fluids (aqueous humor or vitreous). However, since the sensitivity of conventional fungal cultures is not high, and the culture growth rates are slow, longer times are required before final results can be obtained [5, 6]. Thus, an early diagnosis can be important in ensuring there is prompt management of the endophthalmitis. Previous studies have shown that polymerase chain reaction (PCR) can be successfully and reliably used to make a diagnosis of fungal endophthalmitis [7–10]. However, even conventional PCR has yet to be able to determine quantitative information for the fungal genome in ocular samples.

In this study, we used real-time quantitative PCR for detection of *Candida* and *Aspergillus* DNA. We developed a protocol for the rapid detection of fungal DNA in ocular samples that was based on two major species (*Candida* and *Aspergillus*) that commonly cause eye disorders. We designed novel panfungal primers and probes that were complementary to the 18S rRNA sequences present in these species. Our broad-range real-time PCR proved to be an accurate method for quantitating fungal copies of both *Candida* and *Aspergillus* DNA.

Methods

Sample preparation

From 2006 to 2010, we consecutively enrolled endophthalmitis and uveitis patients in a prospective study that was conducted at our hospital (Table 1). After informed consent was obtained in all patients, we collected aqueous humor and vitreous fluid samples. A 0.1–0.2 ml aliquot of aqueous humor (asepsis) was collected in a syringe with a 30-G needle. We also collected non-diluted vitreous fluid samples (0.5–1.0 ml) during diagnostic pars plana vitrectomy (PPV) procedures that were conducted in patients with clinically suspected fungal endophthalmitis/uveitis. All of the patients displayed active intraocular inflammation at the time of sampling. The samples were transferred into a pre-sterilized microfuge tube and used for PCR. To ensure that no contamination of the PCR preparation occurred, the DNA amplification and the analysis of the amplified products were done in separate laboratories, as per a method reported for one of our previous studies [11].

For cultures of fungi, the Bacteria Work Station of the Tokyo Medical and Dental University Hospital processed all specimens (aqueous humor and vitreous fluids) within 1 h after the sample collection, with standard methods followed for the isolation and identification of fungal cultures [11].

In addition to the patient groups, we also analyzed samples from a control group. A total of 40 samples (20 aqueous humor and 20 vitreous fluids) were collected from patients who did not have any type of ocular inflammation (age-related cataract, macular edema, retinal detachment, idiopathic macular hole, or idiopathic epiretinal membrane).

The research followed the tenets of the Declaration of Helsinki and all study protocols were approved by the Institutional Ethics Committee of Tokyo Medical and Dental University. This clinical trial was registered, with registration information available at www.umin.ac.jp/ctr/index/htm. The study number attached to this registration is R000002708. The study was begun in April of 2006 and ended in April of 2010.

Polymerase chain reaction

To detect the *Candida* and *Aspergillus* DNA, we designed primers and probes for the broad-range PCR of the 18S rRNA sequences, which we have described in a previous report [10]. Kami et al. [12] developed primers and a probe for real-time PCR and demonstrated that the procedure was highly specific for the *Aspergillus* infection. In this study, we also designed a probe for use in the *Candida* species DNA amplifications (Fig. 1).

DNA was extracted from the samples using a DNA Mini Kit (Qiagen, Valencia, CA) installed on a robotic workstation that was set for automated purification of nucleic acids (BioRobot E21, Qiagen). The real-time PCR was performed using the Amplitaq Gold and the Real-Time PCR 7300 system (Applied Biosystems, Foster City, CA) or Light Cycler 480 II (Roche, Switzerland). The paired primers and TaqMan probes used for *Candida* and *Aspergillus* are shown in Fig. 1. Products were subjected to 50 cycles of PCR amplification, with cycling conditions set at 95°C for 10 min, followed by 50 cycles at 95°C for 15 s and 60°C for 1 min. For PCR assay sensitivity, PCR fragments were amplified from the DNA of *C. albicans* (Strain: ATCC 60193). Amplification of the human β-globulin gene served as an internal positive extraction and amplification control. Copy number values of more than ten copies/ml in the sample were considered to be significant.

Results

Specificity of *Candida* and *Aspergillus* species in broad-range real-time PCR

To evaluate the specificity of the *Candida* and *Aspergillus* species using broad-range real-time PCR of the 18S rRNA sequences, total nucleic acids of six *Candida* species and five *Aspergillus* species were extracted and assayed for 18S

Table 1 Detection of *Candida* and *Aspergillus* 18S rRNA gene by broad-range real-time PCR in unknown uveitis or endophthalmitis patients and control uveitis patients

Initial diagnosis	No. of patients	Sample	Results for real-time PCR	Final diagnosis	Remarks
Idiopathic uveitis/ endophthalmitis	n=46	Aqh, VF	<10 copies	Idiopathic uveitis/ endophthalmitis	
	n=1 (65, male)	VF	*Candida* 9.2×10^5 copies/ml	*Candida* endophthalmitis	Case 1; Endogenous endophthalmitis
	n=1 (71, female)	VF	*Aspergillus* 4.5×10^2 copies/ml	*Aspergillus* endophthalmitis	Case 2; Endogenous endophthalmitis
	n=1 (73, male)	VF	*Aspergillus* 1.8×10^3 copies/ml	*Aspergillus* endophthalmitis	Case 3; Late postoperative endophthalmitis
	n=1 (80, male)	Aqh	*Candida* 3.4×10^2 copies/ml	*Candida* endophthalmitis	Case 4; Post-traumatic corneal ulceration
	n=1 (66, female)	VF	*Candida* 6.5×10^5 copies/ml	*Candida* endophthalmitis	Case 5; Endogenous endophthalmitis (IFN treatment)
	n=1 (74, male)	VF	*Candida* 6.2×10^4 copies/ml	*Candida* endophthalmitis	Case 6; Endogenous endophthalmitis (diabetes)
	n=1 (0, female)	VF	*Candida* 9.4×10^4 copies/ml	*Candida* endophthalmitis	Case 7; Endogenous endophthalmitis (normal infant)
	n=1 (60, male)	Aqh	<10 copies	*Candida* endophthalmitis	Case 8; Endogenous endophthalmitis (IVH use)
Bacterial endophthalmitis	n=7	Aqh, VF	<10 copies	/	
Sarcoidosis	n=4	Aqh, VF	<10 copies	/	
Vogt-Koyanagi-Harada disease	n=1	Aqh	<10 copies	/	
Toxocariasis	n=1	Aqh	<10 copies	/	
Toxoplasmosis	n=3	Aqh, VF	<10 copies	/	
Acute retinal necrosis	n=7	Aqh, VF	<10 copies	/	
Cytomegalovirus retinitis	n=4	Aqh, VF	<10 copies	/	
Herpetic anterior iridocyclitis	n=4	Aqh	<10 copies	/	
Non-inflammatory ocular diseases*	n=40	Aqh, VF	<10 copies	/	Controls for PCR

*Non-inflammatory ocular diseases: age-related cataract, macular edema, retinal detachment, idiopathic macular hole or idiopathic epiretinal membrane

Aqh aqueous humor, *IFN* interferon, *IVH* Intravenous hyperalimentation, *VF* vitreous fluids

rDNA. As seen in Fig. 1, the broad-range real-time PCR detected six *Candida* species, i.e., *C. albicans, C. parapsilosis, C. tropicalis, C. guilliermondii, C. glabrata,* and *C. krusei*, along with five *Aspergillus* species, i.e., *A. fumigatus, A. flavus, A. nidulans, A. niger,* and *A. terreus*. By using several different primers and probes, we were able to separately detect each of these fungal species (Fig. 1).

Sensitivity of the real-time PCR assay

To confirm the broad-range real-time PCR assay sensitivity, PCR fragments were amplified from the DNA of *C. albicans*. The detection limit and standard range of the TaqMan real-time PCR were determined by using serial tenfold dilutions of linearized plasmid. The PCR results for the prepared samples showed that the best sensitivity for detecting *C. albicans* DNA was at a concentration of 10^1 per PCR (Fig. 2). There was no detection of the DNA in the negative control (nuclease-free water).

Detection of *Candida* and *Aspergillus* 18S rRNA gene in unknown uveitis/endophthalmitis patients

PCR results indicated a total of seven ocular fluid samples from the idiopathic uveitis or endophthalmitis patients (7/54, 13% positive, Table 1) were positive for *Candida* or *Aspergillus* DNA. These positive patients had high copy numbers of either *Candida* or *Aspergillus* DNA, with values ranging from 3.4×10^2 to 9.2×10^5 copies/ml. These results indicate the presence of a fungal infection. A representative PCR result is shown in Fig. 3. Conversely, conventional fungal cultures only found two out of the seven PCR-positive samples (both *C. albicans*) to be positive, while the other five samples were negative.

On the other hand, fungal DNA was not detected in any of the other 46 samples collected from these idiopathic uveitis or endophthalmitis patients. In the one PCR-negative case, PCR did not detect any fungal genome in the aqueous humor (<10 copies, case 8 in Table 1), even

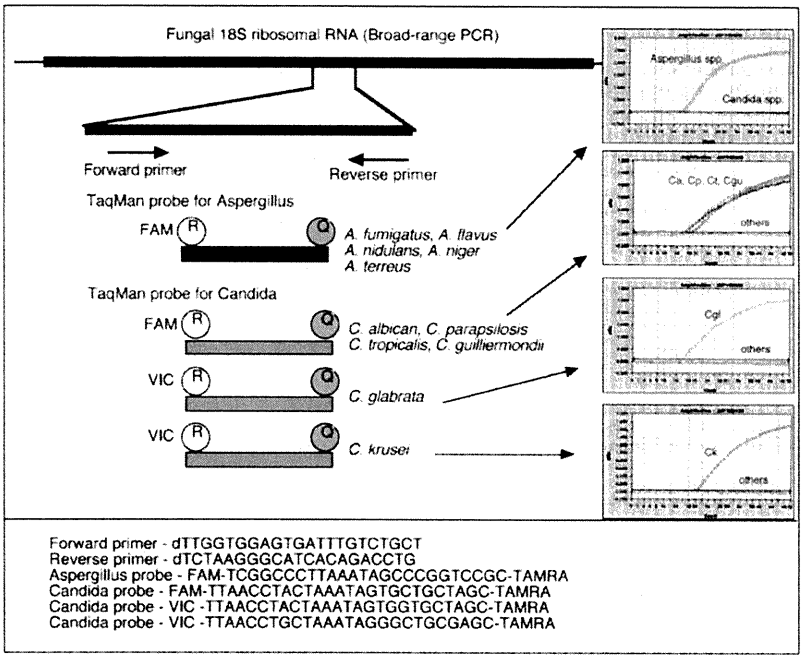

Fig. 1 Specific primers and probes for broad-range real-time PCR of the fungal 18S rRNA sequence were designed in order to detect DNA for *Candida* and *Aspergillus* species

though this patient was clinically suspected of having *Candida* endophthalmitis. Real-time PCR results were negative for the *Candida* and *Aspergillus* DNA in the bacterial endophthalmitis patients (n=7) and in the various uveitis patients (n=24) who had been diagnosed with sarcoidosis, Vogt-Koyanagi-Harada disease, toxocariasis, toxoplasmosis, acute retinal necrosis, cytomegalovirus retinitis, or herpetic anterior iridocyclitis. In addition, fungal DNA was not detected in any of the 40 control samples that were collected from the patients without ocular inflammation.

Of the seven patients who were PCR positive, further examinations led to fungal endophthalmitis diagnoses as follows: five patients had endogenous endophthalmitis (four *Candida* and one *Aspergillus*), one had late postoperative endophthalmitis (*Aspergillus*, case 3), and one had post-traumatic keratitis-associated endophthalmitis (*Candida*, case 4) (Table 1).

Case reports

Case 1

A 65-year-old man with type II diabetes mellitus was treated for unknown uveitis over a period of a few weeks during 2009. He complained of blurred vision, decreased visual acuity, and pain in his right eye (RE). Ophthalmologic examination demonstrated the presence of characteristics of uveitis, bacterial endophthalmitis and fungal endophthalmitis. Vitreous opacity, including the presence of a fungal ball and yellowish retinal exudates, was seen in the fundus of his RE (Fig. 4a). After vitrectomy of his RE,

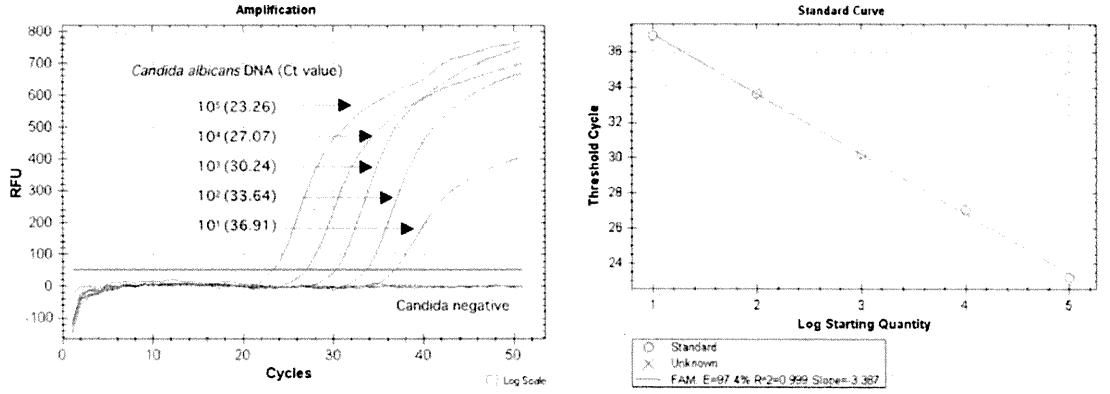

Fig. 2 In order to examine broad-range real-time PCR assay sensitivity for the fungal 18S PCR, the PCR fragments were amplified from the DNA of *C. albicans* (ATCC 60193). The *number in parenthesis* indicates the cycle threshold (Ct) value in quantitative PCR

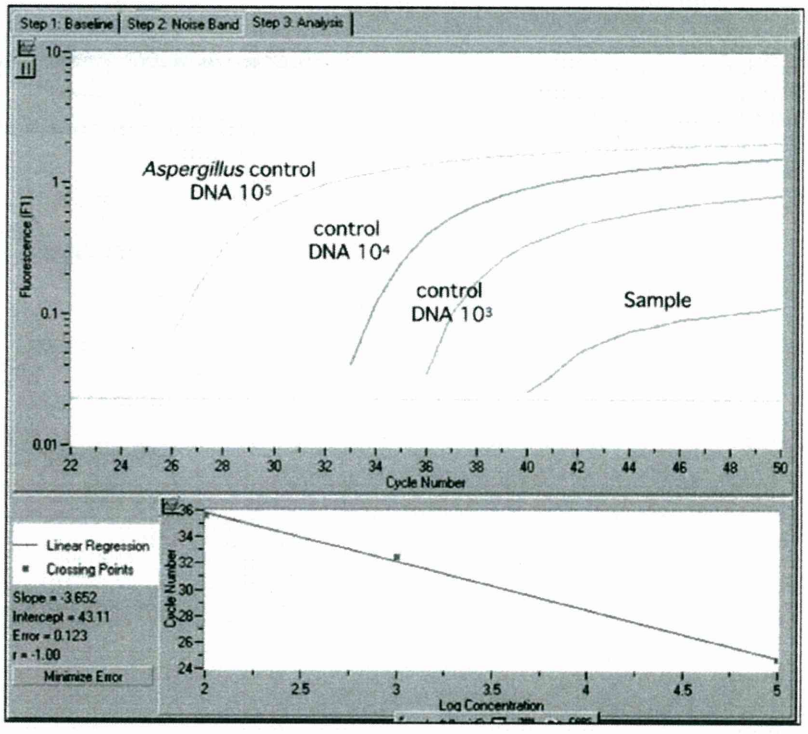

Fig. 3 Representative data for the broad-range real-time PCR. *Aspergillus* DNA (4.5×10^2 copies/ml) but not *Candida* DNA was detected in the vitreous sample of case 2

real-time PCR of the vitreous sample obtained during the procedure indicated there were high copy numbers of *Candida* DNA (9.2×10^5 copies/ml, Fig. 4b). Based on these results, the patient was given systemic fluconazole (Table 1). *Aspergillus* DNA was not detected in this sample. A few days later, fungal culture of his vitreous specimen

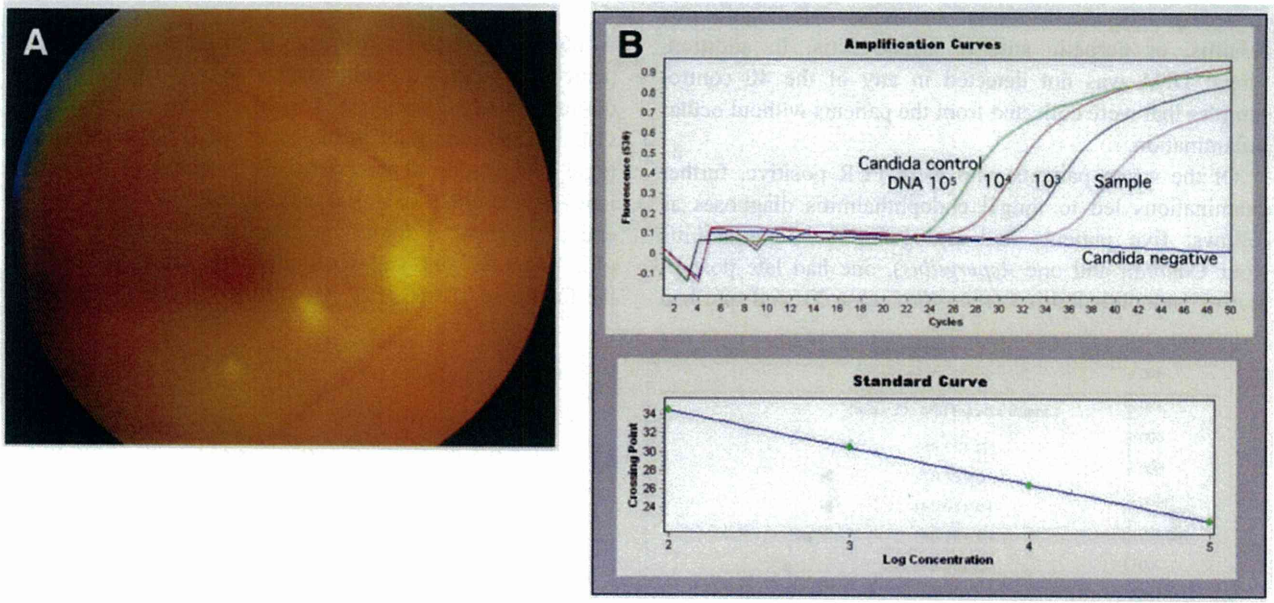

Fig. 4 PCR results for case 1. **a** Fundus photograph of the right eye with a *Candida* infection. Dense vitreous opacity and retinal exudates are seen. **b** This is a graph of the PCR results. We calculated the copy number of fungal genomic DNA in the sample. After we measured both the tested ocular sample and the control DNA (10^5, 10^4, and 10^3 copies/ml) using real-time PCR, we then established the standard curve based on the results of the control DNA. Based on this standard curve, the sample Ct value was used to determine the DNA concentration of the sample. Final copy numbers of genomic DNA in the sample (copies/ml) were calculated based on the obtained sample volume and final dilution volume. High copy numbers of *Candida* DNA (9.2×10^5 copies/ml) were detected by PCR. *Aspergillus* DNA was not detected in the sample

was also found to be positive for *C. albicans*. After being treated, he had complete resolution of his symptoms.

Case 3

A 73-year-old man was referred to the Uveitis Clinic at our hospital in July 2008 because of keratic precipitates (KPs), cells in the anterior chamber, and anterior vitreous opacity in his RE that was associated with recurrent anterior uveitis. In his RE, diffuse pigmented KPs were seen (Fig. 5a). After considering both the clinical features and whole body inspections, we diagnosed this case as idiopathic uveitis. Although he was treated with topical corticosteroid and an antibiotic for 2 months, the KPs expanded (Fig. 5b). During the treatment, diffuse pigmented KPs continued to expand and then united. In addition, we also observed cells in the anterior chamber with hypopyon and dense anterior vitreous opacity. After informed consent was obtained, pars plana vitrectomy was performed in order to obtain a vitreous sample. Although fungi were not detected in a culture test, real-time PCR detected 1.8×10^3 copies/ml of the *Aspergillus* 18S rRNA gene (Table 1). Microbiological investigations performed using both culture and Gram's staining of the vitreous sample proved to be negative. A blood test for β-D-glucan and fungal antigens including *Aspergillus* were also negative. We diagnosed the patient as having *Aspergillus*-associated late postoperative endophthalmitis that was related to his 2007 cataract surgery. The patient was subsequently treated using systemic fluconazole. The medication proved to be effective in treating the infectious endophthalmitis, with the inflammation in the anterior segment of his RE completely disappearing (Fig. 5c). After treatment, *Aspergillus* DNA in his sample was below the PCR detection level.

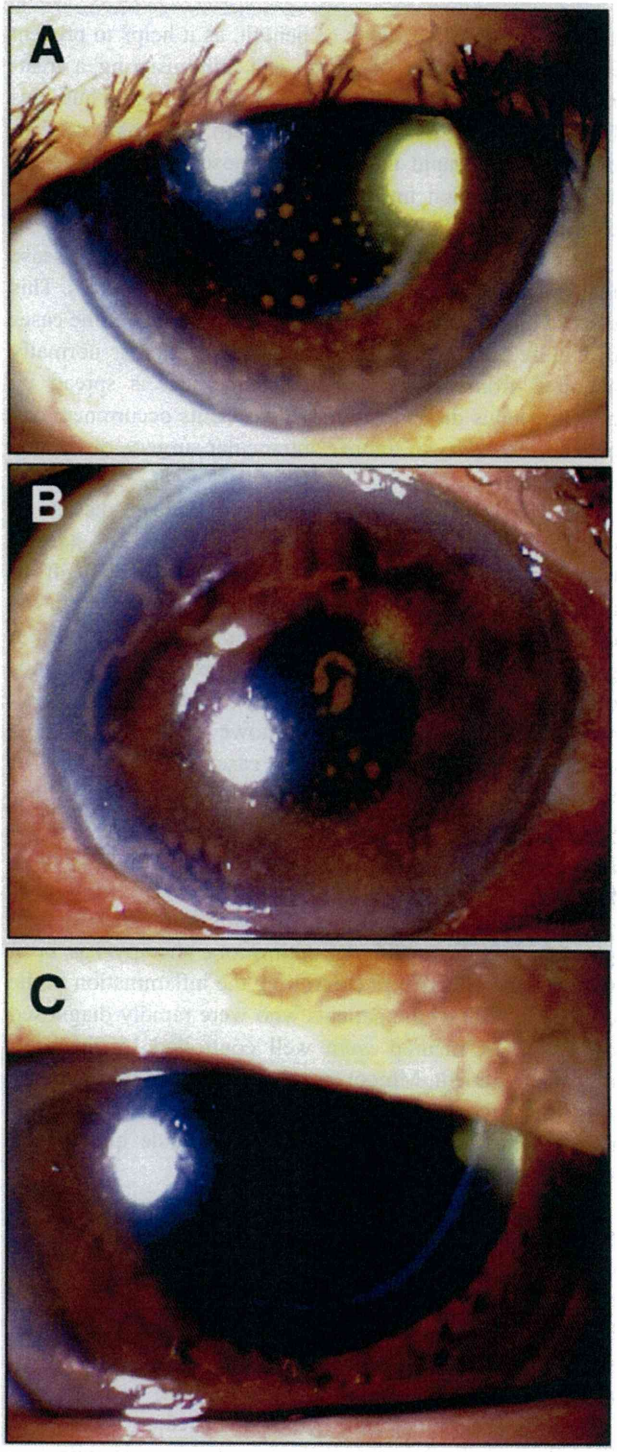

Fig. 5 PCR results for case 3. **a** Slit photograph of the right eye with an *Aspergillus* infection. Diffuse pigmented keratic precipitates (KPs) are seen. **b** The pigmented KPs are expanded and united. Like the previous case, the *Aspergillus* DNA gene (1.8×10^3 copies/ml) but not the *Candida* DNA was detected in the sample. **c** After treatment, the inflammation completely disappeared

Discussion

PCR is well suited for the detection of fungal moieties due to its specificity and applicability for use with small samples such as ocular specimens. Moreover, real-time quantitative PCR can be used to determine whether or not the fungus is related to endophthalmitis. By utilizing our broad-range real-time PCR for the 18S rRNA sequence, we were able to rapidly diagnose *Candida* or *Aspergillus* endophthalmitis in a few patients that exhibited clinical evidence of a fungal infection. While our methodology showed both positive and negative results, it was generally more helpful than waiting for culture results, as the culture tests used to detect *Candida* or *Aspergillus* are both difficult to perform and require longer amounts of time due to the slow growth rates for these species [5, 6, 13]. In addition, the specificity of our PCR examination is good enough so

that even a negative test is of benefit, as it helps to prevent making an incorrect diagnosis and administering a treatment for an infectious agent that is not present. Thus, this broad-range and real-time PCR system for ocular samples can provide a rapid diagnosis for those patients suffering from an unknown intraocular disorder such as idiopathic uveitis or endophthalmitis.

Fungal endophthalmitis is a sight-threatening disease that is most commonly caused by the *Candida* species. This disease usually accounts for a few percent of all of the cases of culture-proven endophthalmitis. The disease is normally acquired from an endogenous source that is spread by hematogenous dissemination. However, its occurrence may also be secondary to trauma, intraocular surgery, or corneal ulceration.

As confirmation of this suspected clinical disease is often difficult, there is frequently a delay in starting treatments. In the present patients, it was difficult to ascertain whether *Candida* or *Aspergillus* species were the causative agent in the intraocular inflammation. Since, in general, all of the patients were elderly and were immunocompetent, there was no focus area for the fungal infection systemically. As seen in Table 1, however, there were three exceptions. These included one case with a history of trauma (case 4), one case with a history of ocular surgery (case 3), and one case involving a normal infant (case 7), and for whom the case report details have been previously published [14].

In cases of fungal endophthalmitis in immunocompetent patients, specific additional antimycotic therapy has been shown to be effective in controlling the inflammation in the eye. In fact, all of the patients who were rapidly diagnosed by this PCR method were well controlled by the antimycotic treatment. Moreover, our PCR system was not only able to detect the conserved sequence of the fungal 18S rRNA gene, but it was also able to provide quantitative information from the ocular samples.

In recent years, PCR technology has been demonstrated to have a great potential in the detection and identification of low copy numbers of a microorganism's DNA in clinical samples [7–12, 15, 16]. It also holds great promise for being able to identify small numbers of organisms in small sample volumes, a situation that is commonly seen when trying to examine intraocular samples from patients with infectious endophthalmitis. We evaluated these PCR techniques in order to determine a reliable and effective protocol for detecting *Candida* or *Aspergillus* species DNA in ocular samples. Our specific aims were to try and significantly increase the number of intraocular samples from which a confirmed diagnosis could be made and to reduce the time it took to make a mycologic diagnosis. In many previous reports, DNAs of *Candida* and *Aspergillus* species were detected in patients with clinically suspected fungal endophthalmitis [7–10, 15–20]. For example, *Candida* species such as *C. albicans*, *C. parapsilosis*, *C. tropicalis*, *C. guilliermondii*, *C. glabrata*, and *C. krusei* have been increasingly recognized as being capable of causing fungal endophthalmitis. However, *C. albicans* has been shown to be the causative agent in the majority of cases of culture-proven endophthalmitis. Moreover, *Aspergillus* such as *A. fumigatus*, *A. flavus*, *A. nidulans*, *A. niger*, and *A. terreus* have also been reported to be the causative species in an unknown ocular infection [17–20]. To detect these fungal species, our present PCR system used paired primers and specific probes that were based upon the 18S rRNA genes of *Candida* and *Aspergillus* (see Fig. 1).

In one patient who was clinically suspected of having *Candida* endophthalmitis, our new PCR method did not detect any fungal genome in the ocular sample (case 8 in Table 1). However, it should be noted that this sample was aqueous humor and not vitreous fluid. Perhaps if a vitreous sample had been obtained, we might have detected *Candida* DNA, as *Candida* endophthalmitis often results from hematogenous dissemination. In fact, this particular patient received intravascular catheters after his initial surgery. Thus, in order to be able to make an accurate diagnosis, the type of sample that is collected may be very important.

Although there are many advantages for using our PCR assay, there is one disadvantage when attempting to diagnose fungal ocular infection. While our PCR examination was able to detect all species of *Candida* and *Aspergillus* DNA, it could not detect other fungi DNA. Recently, Vollmer et al. reported on a novel broad-range real-time PCR assay for the rapid detection of human pathogenic fungi [21]. Their assay targeted a part of the 28S large subunit rRNA (rDNA) gene. Since this PCR assay can examine *Candida* species, *Aspergillus* species, *Cryptococcus* species, among others, we are currently trying to develop a new PCR examination that uses these primers and probes for the diagnosis of fungal ocular infections, including fungal endophthalmitis.

In conclusion, utilization of the PCR assay to examine ocular samples in patients with suspected fungal endophthalmitis and idiopathic uveitis or endophthalmitis appears to be clinically useful for detecting *Candida* and *Aspergillus* DNA. Thus, broad-range PCR for the 18S rRNA sequence is a reliable tool for the diagnosis of fungal endophthalmitis and in screening for fungal infections. Moreover, because real-time PCR is an accurate method of quantitating fungal copies, real-time quantitative PCR can be used to determine whether the fungus is related to the endophthalmitis. Since the sensitivity of conventional culture techniques is not high and these cultures tend to take a long time due to their slow growth, the use of a broad-range and real-time PCR system to analyze ocular samples may be a better way to obtain a rapid diagnosis in

patients suffering from unknown intraocular infectious disorders. As early treatments are also essential for infectious endophthalmitis, this method may help to ensure that patients receive timely and optimal treatments. However, this is currently a limited research tool and not widely available for clinical labs at the present time. As a next step, we will need to work on making these tests widely available to clinical labs as oppose to only having them in research labs. In the near future, it is assumed that a comprehensive PCR system for examining fungi, bacteria, parasites, and viruses will become available, and be able to be used in the diagnosis of ocular infectious disorders.

Acknowledgements We thank Ms. Miki Katayama and Shizu Inoue for their technical assistance. We would like to also thank Drs. Hiroshi Takase and Yoshiharu Sugamoto for obtaining the samples used in this study. This work was supported by a Comprehensive Research on Disability, Health and Welfare grant, along with a Health and Labour Sciences Research Grant from the Ministry of Health, Labour and Welfare, Japan.

No financial relationships exist in the publishing of this work.

References

1. Edwards JE Jr, Foos RY, Montgomerie JZ, Guze LB (1974) Ocular manifestations of *Candida* septicemia: review of seventy-six cases of hematogenous *Candida* endophthalmitis. Medicine 53:47–75
2. Rao NA, Hidayat AA (2001) Endogenous mycotic endophthalmitis: variations in clinical and histopathologic changes in candidiasis compared with aspergillosis. Am J Ophthalmol 132:244–251
3. Klotz SA, Penn CC, Negvesky GJ, Butrus SI (2000) Fungal and parasitic infection of the eye. Clin Microbiol Rev 13:662–685
4. Walsh TJ, Anaissie EJ, Denning DW, Herbrecht R, Kontoyiannis DP, Marr KA, Morrison VA, Segal BH, Steinbach WJ, Stevens DA, van Burik JA, Wingard JR, Patterson TF, Infectious Diseases Society of America (2008) Treatment of aspergillosis; clinical practice guidelines of the Infectious Disease Society of America. Clin Infect Dis 46:327–360
5. Kunimoto DY, Das T, Sharma S, Jalali S, Majji AB, Gopinathan U, Athmanathan S, Rao TN (1999) Microbiologic spectrum and susceptibility of isolates: part I. Postoperative endophthalmitis. Endophthalmitis Research Group. Am J Ophthalmol 128:240–242
6. Puliafito CA, Baker AS, Haaf J, Foster CS (1982) Infectious endophthalmitis. Review of 36 cases. Ophthalmology 89:921–929
7. Lohmann CP, Linde HJ, Reischl U (2000) Improved detection of microorganisms by polymerase chain reaction in delayed endophthalmitis after cataract surgery. Ophthalmology 107:1047–1051
8. Ferrer C, Colom F, Frasés S, Mulet E, Abad JL, Alió JL (2001) Detection and identification of fungal pathogens by PCR and by ITS2 and 5.8S ribosomal DNA typing in ocular infections. J Clin Microbiol 39:2873–2879
9. Anand AR, Madhavan HN, Sudha NV, Therese KL (2001) Polymerase chain reaction in the diagnosis of *Aspergillus* endophthalmitis. Indian J Med Res 114:133–140
10. Jaeger EE, Carroll NM, Choudhury S, Dunlop AA, Towler HM, Matheson MM, Adamson P, Okhravi N, Lightman S (2000) Rapid detection and identification of *Candida*, *Aspergillus*, and *Fusarium* species in ocular samples using nested PCR. J Clin Microbiol 38:2902–2908
11. Sugita S, Shimizu N, Watanabe K, Katayama M, Horie S, Ogawa M, Takase H, Sugamoto Y, Mochizuki M (2011) Diagnosis of bacterial endophthalmitis by broad-range quantitative polymerase chain reaction. Br J Ophthalmol 95:345–349
12. Kami M, Fukui T, Ogawa S, Kazuyama Y, Machida U, Tanaka Y, Kanda Y, Kashima T, Yamazaki Y, Hamaki T, Mori S, Akiyama H, Mutou Y, Sakamaki H, Osumi K, Kimura S, Hirai H (2001) Use of real-time PCR on blood samples for diagnosis of invasive aspergillosis. Clin Infect Dis 33:1504–1512
13. Akler ME, Vellend H, McNeely DM, Walmsley SL, Gold WL (1995) Use of fluconazole in the treatment of *Candida* endophthalmitis. Clin Infect Dis 20:657–664
14. Ito M, Yokoi T, Sugita S, Shinohara N, Nishina S, Azuma N (2010) Endogenous *Candida* chorioretinitis in a healthy infant. Jpn J Ophthalmol 54:629–631
15. Tarai B, Gupta A, Ray P, Shivaprakash MR, Chakrabarti A (2006) Polymerase chain reaction for early diagnosis of post-operative fungal endophthalmitis. Indian J Med Res 123:671–678
16. Hidalgo JA, Alangaden GJ, Eliott D, Akins RA, Puklin J, Abrams G, Vazquez JA (2000) Fungal endophthalmitis diagnosis by detection of *Candida albicans* DNA in intraocular fluid by use of a species-specific polymerase chain reaction assay. J Infect Dis 181:1198–1201
17. Shen X, Xu G (2009) Vitrectomy for endogenous fungal endophthalmitis. Ocul Immunol Inflamm 17:148–152
18. Moinfar N, Smiddy WE, Miller D, Miller D, Herschel K (2007) Posttraumatic *Aspergillus terreus* endophthalmitis masquerading as dispersed lens fragments. J Cataract Refract Surg 33:739–740
19. Kramer M, Kramer MR, Blau H, Bishara J, Axer-Siegel R, Weinberger D (2006) Intravitreal voriconazole for the treatment of endogenous *Aspergillus* endophthalmitis. Ophthalmology 113:1184–1186
20. Kalina PH, Campbell RJ (1991) *Aspergillus terreus* endophthalmitis in a patient with chronic lymphocytic leukemia. Arch Ophthalmol 109:102–103
21. Vollmer T, Störmer M, Kleesiek K, Dreier J (2008) Evaluation of novel broad-range real-time PCR assay for rapid detection of human pathogenic fungi in various clinical specimens. J Clin Microbiol 46:1919–1926

OPEN ACCESS Freely available online PLoS PATHOGENS

Novel Mouse Xenograft Models Reveal a Critical Role of CD4$^+$ T Cells in the Proliferation of EBV-Infected T and NK Cells

Ken-Ichi Imadome[1☯*], Misako Yajima[1☯¤], Ayako Arai[2], Atsuko Nakazawa[3], Fuyuko Kawano[1], Sayumi Ichikawa[1,4], Norio Shimizu[4], Naoki Yamamoto[5¤], Tomohiro Morio[6], Shouichi Ohga[7], Hiroyuki Nakamura[1], Mamoru Ito[8], Osamu Miura[2], Jun Komano[5], Shigeyoshi Fujiwara[1*]

1 Department of Infectious Diseases, National Research Institute for Child Health and Development, Tokyo, Japan, **2** Department of Hematology, Tokyo Medical and Dental University, Tokyo, Japan, **3** Department of Pathology, National Center for Child Health and Development, Tokyo, Japan, **4** Department of Virology, Division of Medical Science, Medical Research Institute, Tokyo Medical and Dental University, Tokyo, Japan, **5** AIDS Research Center, National Institute of Infectious Diseases, Tokyo, Japan, **6** Department of Pediatrics and Developmental Biology, Tokyo Medical and Dental University, Tokyo, Japan, **7** Department of Perinatal and Pediatric Medicine, Graduate School of Medical Sciences, Kyushu University, Fukuoka, Japan, **8** Central Institute for Experimental Animals, Kawasaki, Japan

Abstract

Epstein-Barr virus (EBV), a ubiquitous B-lymphotropic herpesvirus, ectopically infects T or NK cells to cause severe diseases of unknown pathogenesis, including chronic active EBV infection (CAEBV) and EBV-associated hemophagocytic lymphohistiocytosis (EBV-HLH). We developed xenograft models of CAEBV and EBV-HLH by transplanting patients' PBMC to immunodeficient mice of the NOD/Shi-*scid*/IL-2Rγ^{null} strain. In these models, EBV-infected T, NK, or B cells proliferated systemically and reproduced histological characteristics of the two diseases. Analysis of the TCR repertoire expression revealed that identical predominant EBV-infected T-cell clones proliferated in patients and corresponding mice transplanted with their PBMC. Expression of the EBV nuclear antigen 1 (EBNA1), the latent membrane protein 1 (LMP1), and LMP2, but not EBNA2, in the engrafted cells is consistent with the latency II program of EBV gene expression known in CAEBV. High levels of human cytokines, including IL-8, IFN-γ, and RANTES, were detected in the peripheral blood of the model mice, mirroring hypercytokinemia characteristic to both CAEBV and EBV-HLH. Transplantation of individual immunophenotypic subsets isolated from patients' PBMC as well as that of various combinations of these subsets revealed a critical role of CD4$^+$ T cells in the engraftment of EBV-infected T and NK cells. In accordance with this finding, in vivo depletion of CD4$^+$ T cells by the administration of the OKT4 antibody following transplantation of PBMC prevented the engraftment of EBV-infected T and NK cells. This is the first report of animal models of CAEBV and EBV-HLH that are expected to be useful tools in the development of novel therapeutic strategies for the treatment of the diseases.

Citation: Imadome K-I, Yajima M, Arai A, Nakazawa A, Kawano F, et al. (2011) Novel Mouse Xenograft Models Reveal a Critical Role of CD4$^+$ T Cells in the Proliferation of EBV-Infected T and NK Cells. PLoS Pathog 7(10): e1002326. doi:10.1371/journal.ppat.1002326

Editor: Shou-Jiang Gao, University of Texas Health Science Center San Antonio, United States of America

Received January 27, 2011; **Accepted** September 2, 2011; **Published** October 20, 2011

Funding: This study was supported by grants from the Ministry of Health, Labour and Welfare of Japan (H22-Nanchi-080 and H22-AIDS-002), the Grant of National Center for Child Health and Development (22A-9), a grant for the Research on Publicly Essential Drugs and Medical Devices from The Japan Health Sciences Foundation (KHC1014), and the Grant-in-Aid for Scientific Research (C) (H22-22590374). The funders had no role in study design, data collection and analysis, decision to publish, or preparation of the manuscript.

Competing Interests: The authors have declared that no competing interests exist.

* E-mail: imadome@nch.go.jp (KI); shige@nch.go.jp (SF)

¤ Current address: Department of Microbiology, Yong Loo Lin School of Medicine, National University of Singapore, Singapore

☯ These authors contributed equally to this work.

Introduction

Epstein-Barr virus (EBV) is a ubiquitous γ-herpesvirus that infects more than 90% of the adult population in the world. EBV is occasionally involved in the pathogenesis of malignant tumors, such as Burkitt lymphoma, Hodgkin lymphoma, and nasopharyngeal carcinoma, along with the post-transplantation lymphoproliferative disorders in immunocompromised hosts. Although EBV infection is asymptomatic in most immunologically competent hosts, it sometimes causes infectious mononucleosis (IM), when primarily infecting adolescents and young adults [1]. EBV infects human B cells efficiently in vitro and transform them into lymphoblastoid cell lines (LCLs) [2]. Experimental infection of T and NK cells, in contrast, is practically impossible except in limited conditions [3,4]. Nevertheless, EBV has been consistently demonstrated in T or NK cells proliferating monoclonally or oligoclonally in a group of diseases including chronic active EBV infection (CAEBV) and EBV-associated hemophagocytic lymphohistiocytosis (EBV-HLH) [5,6,7,8,9,10]. CAEBV, largely overlapping the systemic EBV$^+$ T-cell lymphoproliferative diseases of childhood defined in the WHO classification of lymphomas [11], is characterized by prolonged or relapsing IM-like symptoms, unusual patterns of antibody responses to EBV, and elevated EBV DNA load in the peripheral blood [12,13,14]. CAEBV has a chronic time course with generally poor prognosis; without a proper treatment by hematopoietic stem cell transplantation, the

Author Summary

Epstein-Barr virus (EBV) is a ubiquitous human herpesvirus that infects more than 90% of the adult human population in the world. EBV usually infects B lymphocytes and does not produce symptoms in infected individuals, but in rare occasions it infects T or NK lymphocytes and causes severe diseases such as chronic active EBV infection (CAEBV) and EBV-associated hemophagocytic lymphohistiocytosis (EBV-HLH). We developed mouse models of these two human diseases in which EBV-infected T or NK lymphocytes proliferate in mouse tissues and reproduce human pathologic conditions such as overproduction of small proteins called "cytokines" that produce inflammatory responses in the body. These mouse models are thought to be very useful for the elucidation of the pathogenesis of CAEBV and EBV-HLH as well as for the development of therapeutic strategies for the treatment of these diseases. Experiments with the models demonstrated that a subset of lymphocytes called CD4-positive lymphocytes are essential for the proliferation of EBV-infected T and NK cells. This result implies that removal of CD4-positive lymphocytes or suppression of their functions may be an effective strategy for the treatment of CAEBV and EBV-HLH.

majority of cases eventually develop malignant lymphoma of T or NK lineages, multi-organ failure, or other life-threatening conditions. Monoclonal or oligoclonal proliferation of EBV-infected T and NK cells, an essential feature of CAEBV, implies its malignant nature, but other characteristics of CAEBV do not necessarily support this notion. For example, EBV-infected T or NK cells freshly isolated from CAEBV patients, as well as established cell lines derived from them, do not have morphological atypia and do not engraft either in nude mice or *scid* mice (Shimizu, N., unpublished results). Clinically, CAEBV has a chronic time course and patients may live for many years without progression of the disease [15]. Although patients with CAEBV do not show signs of explicit immunodeficiency, some of them present a deficiency in NK-cell activity or in EBV-specific T-cell responses, implying a role for subtle immunodeficiency in its pathogenesis [16,17,18].

EBV-HLH is the most common and the severest type of virus-associated HLH and, similar to CAEBV, characterized by monoclonal or oligoclonal proliferation of EBV-infected T (most often $CD8^+$ T) cells [5,6]. Clinical features of EBV-HLH include high fever, pancytopenia, coagulation abnormalities, hepatosplenomegaly, liver dysfunction, and hemophagocytosis [19]. Overproduction of cytokines by EBV-infected T cells as well as by activated macrophages and T cells reacting to EBV is thought to play a central role in the pathogenesis [20]. Although EBV-HLH is an aggressive disease requiring intensive clinical interventions, it may be cured, in contrast to CAEBV, by proper treatment with immunomodulating drugs [21]. No appropriate animal models have been so far developed for either CAEBV or EBV-HLH.

NOD/Shi-*scid*/IL-2Rγ^{null} (referred here as NOG) is a highly immunodeficient mouse strain totally lacking T, B, and NK lymphocytes, and transplantation of human hematopoietic stem cells to NOG mice results in reconstitution of human immune system components, including T, B, NK cells, dendritic cells, and macrophages [22,23]. These so called humanized mice have been utilized as animal models for the infection of certain human viruses targeting the hemato-immune system, including human immunodeficiency virus 1 (HIV-1) and EBV [24,25,26,27,28,29,30]. Xenotransplantation of human tumor cells to NOG mice also provided model systems for several hematologic malignancies [31,32,33]. To facilitate investigations on the pathogenesis of CAEBV and EBV-HLH and assist the development of novel therapeutic strategies, we generated mouse models of these two EBV-associated diseases by transplanting NOG mice with PBMC isolated from patients with the diseases. In these models, EBV-infected T, NK, or B cells engrafted in NOG mice and reproduced lymphoproliferative disorder similar to either CAEBV or EBV-HLH. Further experiments with the models revealed a critical role of $CD4^+$ T cells in the in vivo proliferation of EBV-infected T and NK cells.

Results

Engraftment of EBV-infected T and NK cells in NOG mice following xenotransplantation with PBMC of CAEBV patients

Depending on the immunophenotypic subset in which EBV causes lymphoproliferation, CAEBV is classified into the T-cell and NK-cell types, with the former being further divided into the CD4, CD8, and γδT types. The nine patients with CAEBV examined in this study are characterized in Table 1 and include all these four types. Intravenous injection of $1-4\times10^6$ PBMC isolated from these nine patients resulted in successful engraftment of EBV-infected T or NK cells in NOG mice in a reproducible manner (Table 1). The results with the patient 1 (CD4 type), patient 3 (CD8 type), patient 5 (γδT type), and patient 9 (NK type) are shown in Figure 1. Seven to nine weeks post-transplantation, EBV DNA was detected in the peripheral blood of recipient mice and reached the levels of 10^5–10^8 copies/μg DNA (Figure 1A). By contrast, no engraftment of EBV-infected cells was observed when immunophenotypic fractions containing EBV DNA were isolated from PBMC and injected to NOG mice (Figure 1A and Table 2). An exception was the $CD4^+$ T-cell fraction isolated from patients with the CD4 type CAEBV, that reproducibly engrafted when transplanted without other components of PBMC (Figure 1A, Table 2). Flow cytometry revealed that the major population of engrafted cells was either $CD4^+$, $CD8^+$, TCRγδor $CD16^+CD56^+$, depending on the type of the donor CAEBV patient (Figure 1B). EBV-infected cells of identical immunophenotypes were found in the patients and the corresponding mice that received their respective PBMC (Figure 1B). Although human cells of multiple immunophenotypes were present in most recipient mice, fractionation by magnetic beads-conjugated antibodies and subsequent real-time PCR analysis detected EBV DNA only in the predominant immunophenotypes that contained EBV DNA in the original patients (Figure 1B, Table 1). The EBV DNA load observed in individual lymphocyte subsets in the patient 3 and a mouse that received her PBMC is shown as supporting data (Table S1). When PBMC from three healthy EBV-carriers were injected intravenously to NOG mice, as controls, no EBV DNA was detected from either the peripheral blood, spleen, or liver (data not shown). Histological analyses of the spleen and the liver of these control mice identified no EBV-encoded small RNA (EBER)-positive cells, although some CD3-positive human T cells were observed (Figure S2). Analysis of TCR Vβ repertoire demonstrated an identical predominant T-cell clone in patients (patients 1 and 3) and the corresponding mice that received their PBMC (Figure 1C). The general condition of most recipient mice deteriorated gradually in the observation period of eight to twelve weeks, with loss of body weight (Figure S1), ruffled hair, and inactivity.

NOG mice engrafted with EBV-infected T or NK cells were sacrificed for pathological and virological analyses between eight

Table 1. Patients with EBV-T/NK LPD and the results of xenotransplantation of their PBMC to NOG mice.

Patient number	Diagnosis	Sex	Age	Type of infected cells	[1]EBV DNA load in the patients	[2]Engrafted cells in mice	[3]Engraftment	[1]EBV DNA load in mice
1	CAEBV	F	25	CD4	9.2×10^5	CD4, CD8	3/3	$1.0\sim3.8\times10^7$
2	CAEBV	M	46	CD4	$1.3\sim7.2\times10^5$	CD4, CD8	2/2, 3/3	$2.6\sim10\times10^5$
3	CAEBV	F	35	CD8	$2.1\sim78\times10^5$	CD8, CD4	2/2, 2/2	$1.1\sim33\times10^6$
4	CAEBV	M	28	CD8	8.2×10^5	CD8, CD4	3/3	$1.1\sim2.5\times10^6$
5	CAEBV	M	10	γδT	2.2×10^6	γδT, CD4, CD8	2/2	$3.8\sim6.5\times10^6$
6	CAEBV	F	15	γδT	6.2×10^5	γδT, CD4, CD8	2/2	$2.2\sim11\times10^5$
7	CAEBV	M	13	NK	$1.1\sim6.7\times10^5$	NK, CD4, CD8	2/2, 2/2	$0.6\sim15\times10^4$
8	CAEBV	F	13	NK	6.3×10^6	NK, CD4, CD8	3/3, 2/2	$0.8\sim1.9\times10^5$
9	CAEBV	M	8	NK	$1.2\sim8.7\times10^5$	NK, CD4, CD8	2/2, 3/3	$1.8\sim7.2\times10^5$
10	EBV-HLH	M	10	CD8	$2.8\sim38\times10^4$	CD8, CD4	2/2, 2/2	$6.5\sim9.9\times10^4$
11	EBV-HLH	M	50	CD8	6.2×10^5	CD8, CD4	4/4	$7.0\sim45\times10^4$
12	EBV-HLH	M	1	CD8	3.1×10^5	CD8, CD4	2/2	$6.0\sim9.1\times10^4$
13	EBV-HLH	M	64	CD8	$3.2\sim3.9\times10^5$	CD8, CD4	2/2, 2/2	$5.0\sim30\times10^5$

[1]EBV DNA copies/μg DNA in the peripheral blood.
[2]EBV DNA was detected only in the cells of the underlined subsets.
[3]Number of mice with successful engraftment per number of recipient mice is shown for each experiment.
doi:10.1371/journal.ppat.1002326.t001

and twelve weeks post-transplantation. On autopsy, the majority of mice presented with splenomegaly, with slight hepatomegaly in occasional cases (Figure 2A). Histopathological findings obtained from a representative mouse (recipient of PBMC from the patient 3 (CD8 type)) are shown in Figure 2B and reveal infiltration of human $CD3^+CD20^-$ cells to major organs, including the spleen, liver, lungs, kidneys, and small intestine. These cells were positive for both EBER and human CD45RO, indicating that they are EBV-infected human T cells (Figure 2B). In contrast, no EBV-infected T cells were found in mice transplanted with PBMC isolated from a normal EBV carrier (Figure S2). Histopathology of a control NOG mouse is shown in Figure S2. Morphologically, EBV-infected cells are relatively small and do not have marked atypia. The infiltration pattern was leukemic and identical with chronic active EBV infection in children [34]. The architecture of the organs was well preserved in spite of marked lymphoid infiltration. The spleen showed marked expansion of periarterial lymphatic sheath owing to lymphocytic infiltration. In the liver, a dense lymphocytic infiltration was observed in the portal area and in the sinusoid. The lung showed a picture of interstitial pneumonitis and the lymphocytes often formed nodular aggregations around bronchioles and arteries. In the kidney, dense lymphocytic infiltration caused interstitial nephritis. In the small intestine, mild lymphoid infiltration was seen in mucosa. Quantification of EBV DNA in the spleen, liver, lymph nodes, lungs, kidneys, adrenals, and small intestine of this mouse revealed EBV DNA at the levels of $1.5\sim5.1\times10^7$ copies/μg DNA. Mice transplanted with PBMC derived from CAEBV of other types exhibited similar infiltration of EBV-infected T or NK cells to the spleen, liver, and other organs (Figure 2C and data not shown).

EBV-infected T- and NK-cell lines established from CAEBV patients do not engraft in NOG mice

We established EBV-positive cell lines of $CD4^+$ T, $CD8^+$ T, γδT, and $CD56^+$ NK lineages from PBMC of the patients listed in Table 1 by the method described previously [35], and confirmed by flow cytometry that the surface phenotypes of EBV-infected cells in the original patients were retained in these cell lines (data not shown). To test whether these cell lines engraft in NOG mice, $1\sim4\times10^6$ cells were injected intravenously to NOG mice. The results are shown in Figure 3A and indicate that CAEBV-derived cell lines of the $CD8^+$ T, γδT, and $CD56^+$ NK phenotypes do not engraft in NOG mice. Neither human CD45-positive cells nor EBV DNA were detected in the peripheral blood of the mice up to twelve weeks post-transplantation. When the recipient mice were sacrificed at twelve weeks post-injection, no EBV DNA could be detected in the spleen, liver, bone marrow, mesenteric lymph nodes, and kidneys. In contrast, the $CD4^+$ T cell lines derived from the CD4-type patients 1 and 2 engrafted in NOG mice and induced T lymphoproliferation similar to that induced by PBMC isolated freshly from these patients (Figure 3A and data not shown). These results, together with the results of transplantation with EBV-containing subsets of PBMC, indicate that EBV-infected T and NK cells, with the exception of those of the $CD4^+$ subset, are not able to engraft in NOG mice, when they are separated from other components of PBMC, suggesting that some components of PBMC are essential for the outgrowth EBV-infected T and NK cells in NOG mice.

Engraftment of EBV-infected T and NK cells in NOG mice requires $CD4^+$ T cells

To identify the cellular component required for the engraftment of EBV-infected T and NK cells in NOG mice, we transplanted PBMC of CAEBV patients after removing individual immunophenotypic subsets by magnetic beads-conjugated antibodies. The results are shown in Figure 3B and summarized in Table 2. With respect to the patients 3 and 4, in whom $CD8^+$ T cells are infected with EBV, removal of $CD8^+$ cells from PBMC, as expected, resulted in the failure of engraftment, whereas elimination of $CD19^+$, $CD56^+$, or $CD14^+$ cells did not affect engraftment. Importantly, elimination of $CD4^+$ cell fraction, that did not contain EBV DNA, resulted in the failure of engraftment of EBV-infected T cells (Figure 3B and data not shown). In the experiments with the patients 5 and 6, in whom γδT cells were infected, removal $CD4^+$ cells that did not contain EBV DNA, as well as that of γδT cells, resulted in the failure of engraftment.

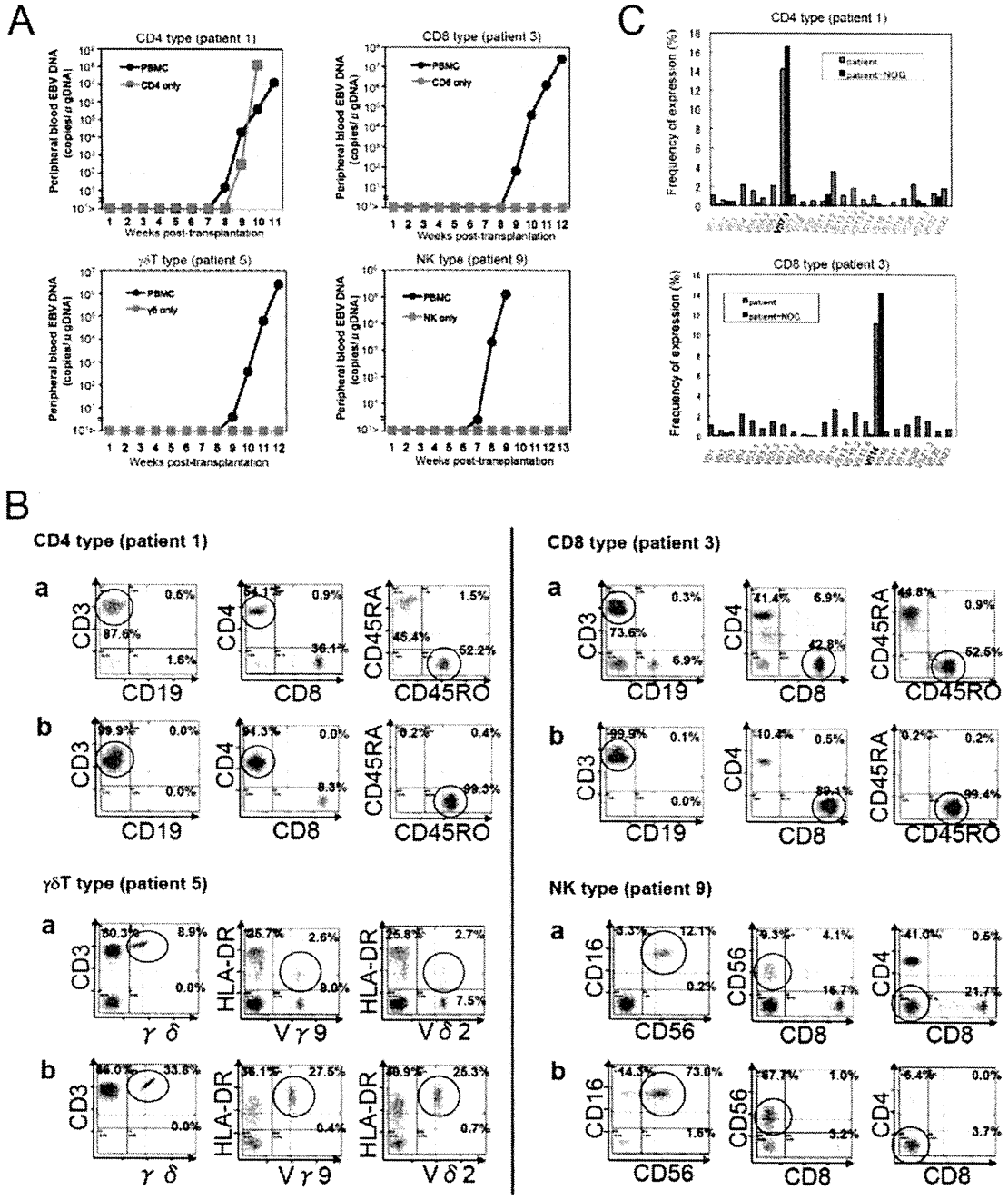

Figure 1. Engraftment of EBV-infected T or NK cells in NOG mice following transplantation with PBMC of patients with CAEBV. A. Measurement of EBV DNA levels. PBMC obtained from the CAEBV patients 1 (CD4 type), 3 (CD8 type), 5 (γδT type), and 9 (NK type) were injected intravenously to NOG mice and EBV DNA load in their peripheral blood was measured weekly by real-time PCR. The results of transplantation with whole PBMC or with isolated EBV DNA-containing cell fraction are shown. B. Flow-cytometric analysis on the expression of surface markers in the peripheral blood lymphocytes of patients (a) with CAEBV and NOG mice (b) that received PBMC from them. Human lymphocytes gated by the pattern of side scatter and human CD45 expression were further analyzed for the expression of various surface markers indicated in the figures. The results from the patients 1, 3, 5, and 9, and the corresponding mice that received their respective PBMC are shown. Circles indicate the fractions that contained EBV DNA. C. Analysis on the expression of TCR Vβ repertoire. Peripheral blood lymphocytes obtained from the patients 1 (CD4 type) and 3 (CD8 type), and from the corresponding mice that received their respective PBMC were analyzed for the expression of Vβ alleles. The percentages of T cells expressing each Vβ allele are shown for the patients (grey bars) and the mice (black bars).
doi:10.1371/journal.ppat.1002326.g001

Removal of $CD8^+$, $CD14^+$, $CD19^+$, or $CD56^+$ cells did not have an influence on the engraftment (Figure 3B and data not shown). Regarding the patients 8 an 9 in whom EBV resided in $CD56^+$ NK cells, removal of $CD4^+$ as well as $CD56^+$ cells resulted in the failure of engraftment, whereas that of $CD8^+$, $CD19^+$, or $CD14^+$ cells did not affect engraftment (Figure 3B and data not shown). In

Table 2. Results of xenotransplantation with subsets of PBMC obtained from CAEBV patients.

Number of patient	Diagnosis	Phenotype of infected cells	Cell fraction transplanted	Number of transplanted cells	Engraftment
1	CAEBV	CD4	PBMC	2×10^6	+
			CD4	2×10^6	+
			PBMC-CD4	3×10^6	−
			PBMC-CD8	2×10^6	+
			PBMC-CD56	2×10^6	+
			PBMC-CD14	2×10^6	+
			PBMC-CD19	2×10^6	+
3	CAEBV	CD8	PBMC	2×10^6	+
			CD8	3×10^6	−
			PBMC-CD4	3×10^6	−
			PBMC-CD8	3×10^6	−
			PBMC-CD56	2×10^6	+
			PBMC-CD14	2×10^6	+
			PBMC-CD19	2×10^6	+
5	CAEBV	γδT	PBMC	2×10^6	+
			γδT	3×10^6	−
			PBMC-CD4	3×10^6	−
			PBMC-γδT	3×10^6	−
			PBMC- CD8	3×10^6	+
			PBMC-CD56	3×10^6	+
			PBMC-CD14	3×10^6	+
			PBMC-CD19	3×10^6	+
9	CAEBV	NK	PBMC	2×10^6	+
			NK	3×10^6	−
			PBMC-CD4	3×10^6	−
			PBMC-CD8	3×10^6	+
			PBMC-CD56	3×10^6	−
			PBMC-CD14	3×10^6	+
			PBMC-CD19	3×10^6	+
11	EBV-HLH	CD8	PBMC	2×10^6	+
			PBMC-CD4	4×10^6	−

doi:10.1371/journal.ppat.1002326.t002

the patients 1 and 2, in whom $CD4^+$ T cells were infected, only the removal of $CD4^+$ cells blocked the engraftment of EBV-infected cells and depletion of either $CD8^+$, $CD19^+$, or $CD14^+$ cells had no effect (Figure 3B and data not shown). These results suggested that EBV-infected cells of the $CD8^+$, γδT, and $CD56^+$ lineages require $CD4^+$ cells for their engraftment in NOG mice. To confirm this interpretation, we performed complementation experiments, in which EBV-containing fractions of the $CD8^+$ (patient 4), γδT (patient 5), or $CD56^+$ (patient 7) phenotypes were transplanted together with autologous $CD4^+$ cells. The results are shown in Figure 3A and indicate that EBV-infected $CD8^+$, γδT, or $CD56^+$ cells engraft in NOG mice when transplanted together with $CD4^+$ cells. Similarly, when EBV-infected cell lines of the $CD8^+$, γδT, and $CD16^+$ lineages were injected intravenously to NOG mice together with autologous $CD4^+$ cells, these cell lines engrafted to the mice (Figure 3A). Finally, to further confirm the essential role of $CD4^+$ cells, we examined the effect of the OKT-4 antibody that depletes $CD4^+$ cells in vivo [24]. PBMC isolated from the CAEBV patient 3 (CD8 type) and the patient 8 (NK type) were injected intravenously to NOG mice and OKT-4 was administered intravenously for four consecutive days starting from the day of transplantation. The results are shown in Figure 4 and indicate that OKT-4 can strongly suppress the engraftment of EBV-infected T and NK cells. In the mice treated with OKT-4, no splenomegaly was observed and EBV DNA was not detected either in the peripheral blood, spleen, liver, or lungs at eight weeks post-transplantation.

Analysis on the EBV gene expression associated with T or NK lymphoproliferation in NOG mice

Previous analysis of EBV gene expression in patients with CAEBV revealed the expression of EBNA1, LMP1, and LMP2A with the involvement of the Q promoter in the EBNA genes transcription and no expression of EBNA2, being consistent with the latency II type of EBV gene expression [36,37,38]. To test whether EBV-infected T and NK cells that proliferate in NOG mice retain this type of viral gene expression, we performed RT-PCR analysis in the spleen and the liver of mice that received

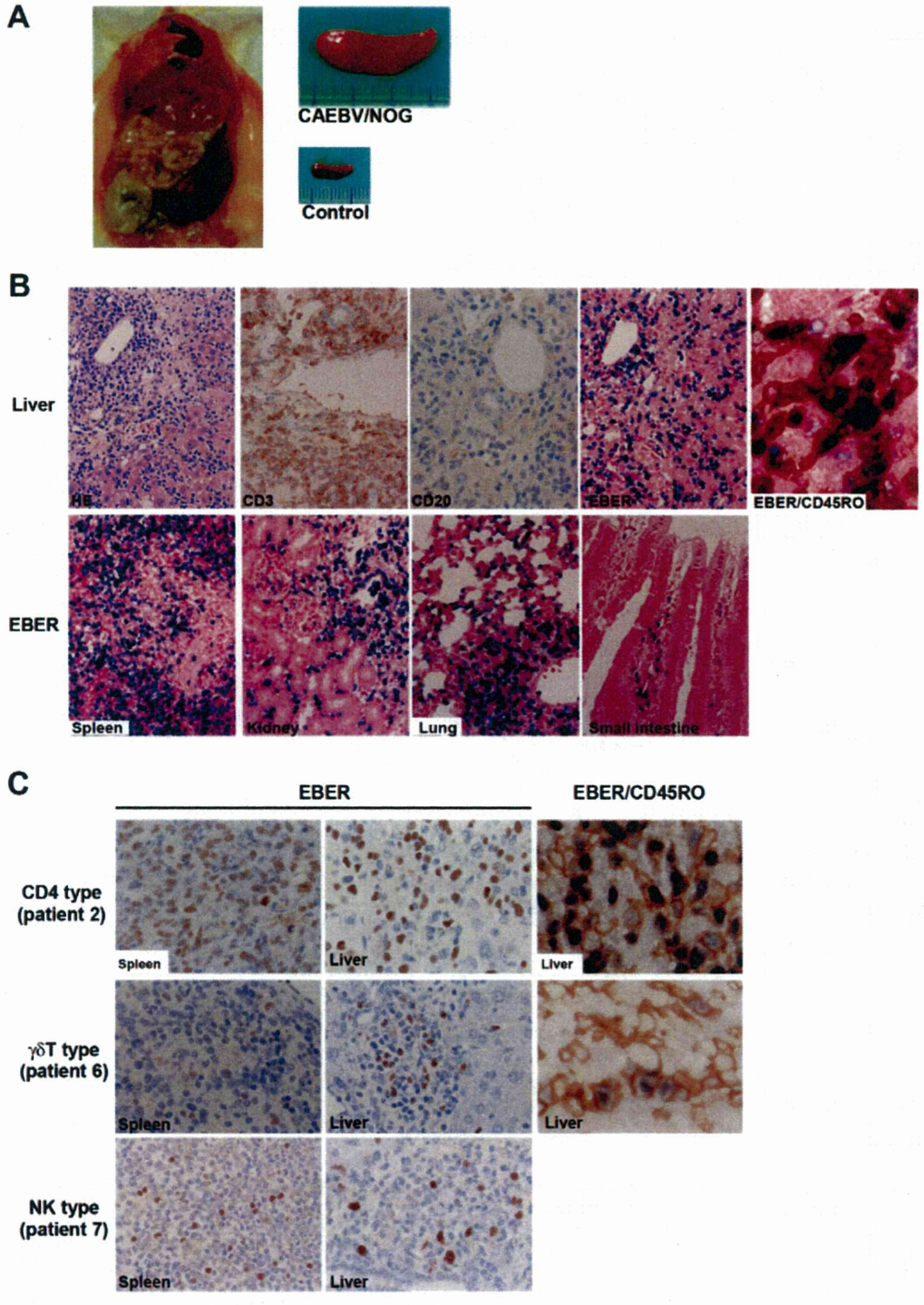

Figure 2. Pathological and immunochemical analyses on NOG mice transplanted with PBMC from CAEBV patients. A. Photographs of a model mouse showing splenomegaly and of the excised spleen. This mouse was transplanted with PBMC from the CAEBV patient 3 (CD8 type). Spleen from a control NOG mouse is also shown. B. Photomicrographs of various tissues of a mouse that received PBMC from the patient 3 (CD8 type). Upper panels: liver tissue was stained with hematoxylin-eosin (HE), antibodies specific to human CD3 or CD20, or by ISH with an EBER probe; the rightmost panel is a double staining with EBER and human CD45RO. Bottom panels: EBER ISH in the spleen, kidney, lung, and small intestine. Original magnification is ×200, except for EBER/CD45RO, that is ×400. C. Photomicrographs of the spleen and liver tissues obtained from NOG mice transplanted with PBMC from the CAEBV patients 2 (CD4 type), 6 (γδT type) or 7 (NK type). Tissues were stained by EBER-ISH or by double staining with EBER-ISH and human CD45RO. Original magnification ×600.
doi:10.1371/journal.ppat.1002326.g002

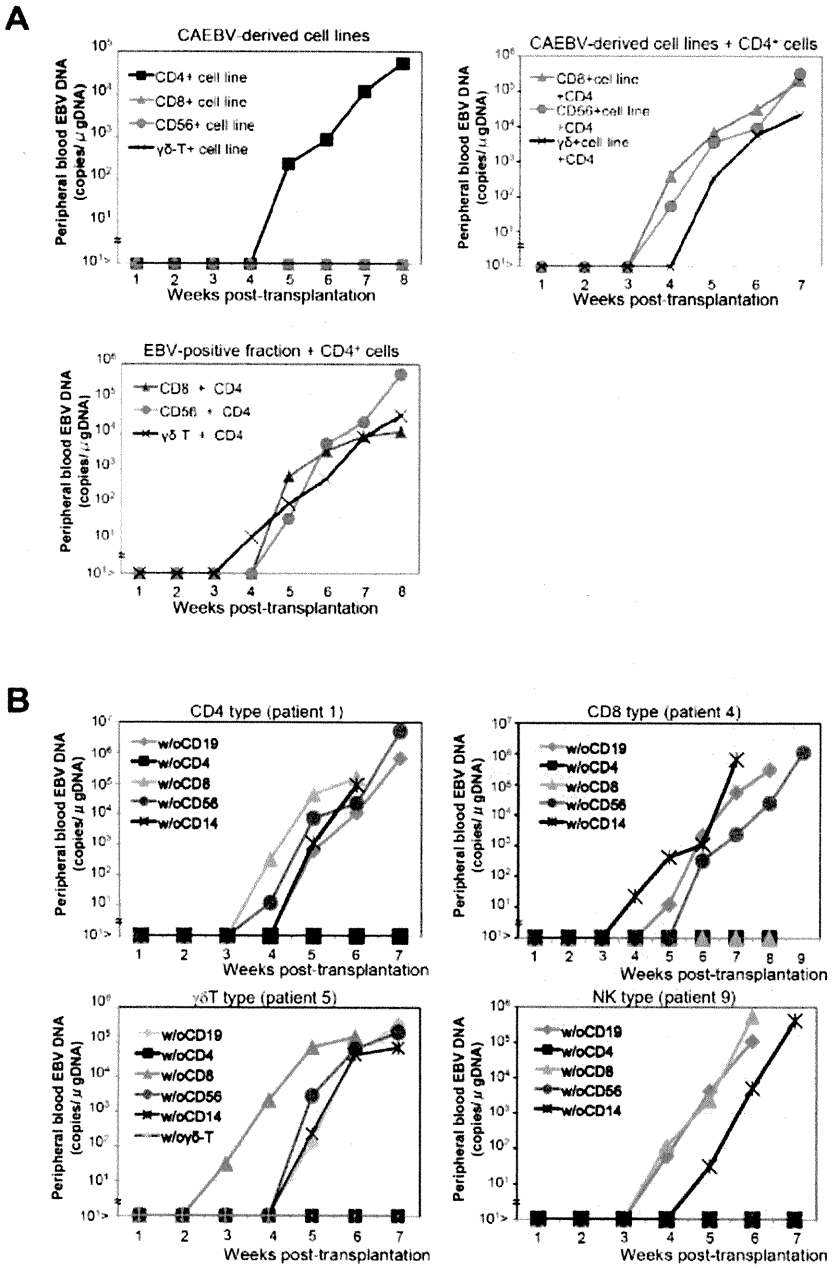

Figure 3. Analysis on the conditions of the engraftment of EBV-infected T and NK cells in NOG mice. A. EBV-infected T or NK cells isolated from patients with CAEBV or cell lines derived from them were injected to NOG mice in the conditions described below. Peripheral blood EBV DNA levels were then measured weekly. Upper-left panel: 5×10^6 cells of EBV-infected $CD4^+$ T, $CD8^+$ T, γδT, and $CD56^+$ NK cell lines established from the CAEBV patients 1, 4, 6, and 8, respectively, were injected intravenously to NOG mice. Upper-right panel: 5×10^6 cells of the $CD8^+$ T, γδT, and $CD56^+$ NK cell lines established from the patients 3, 6, and 8, respectively, were injected intravenously to NOG mice together with autologous $CD4^+$ T cells isolated from 5×10^6 PBMC. Bottom panel: 5×10^6 cells of the $CD8^+$ T, γδT, and $CD56^+$ NK fractions isolated freshly from the patients 4, 5, and 7, respectively, were injected intravenously to NOG mice together with autologous $CD4^+$ T cells isolated from 5×10^6 PBMC. B. Transplantation of PBMC devoid of individual immunophenotypic subsets to NOG mice. $CD19^+$, $CD4^+$, $CD8^+$, $CD56^+$, or $CD14^+$ cells were removed from PBMC obtained from the patient 1 (CD4 type, upper-left panel), 4 (CD8 type, upper-right), 5 (γδT type, bottom-left), and 9 (NK type, bottom-right) and the remaining cells were injected intravenously to NOG mice. Thereafter peripheral blood EBV DNA was determined weekly.
doi:10.1371/journal.ppat.1002326.g003

PBMC from the CAEBV patient 3 (CD8 type). The results are shown in Figure 5A and demonstrate the expression of mRNAs coding for EBNA1, LMP1, LMP2A, and LMP2B, but not for EBNA2. Expression of the EBV-encoded small RNA 1 (EBER1) was also demonstrated. EBNA1 mRNAs transcribed from either the Cp promoter or the Wp promoter were not detected, whereas those transcribed from the Q promoter was abundantly detected. These results indicate that EBV-infected T cells retain the latency

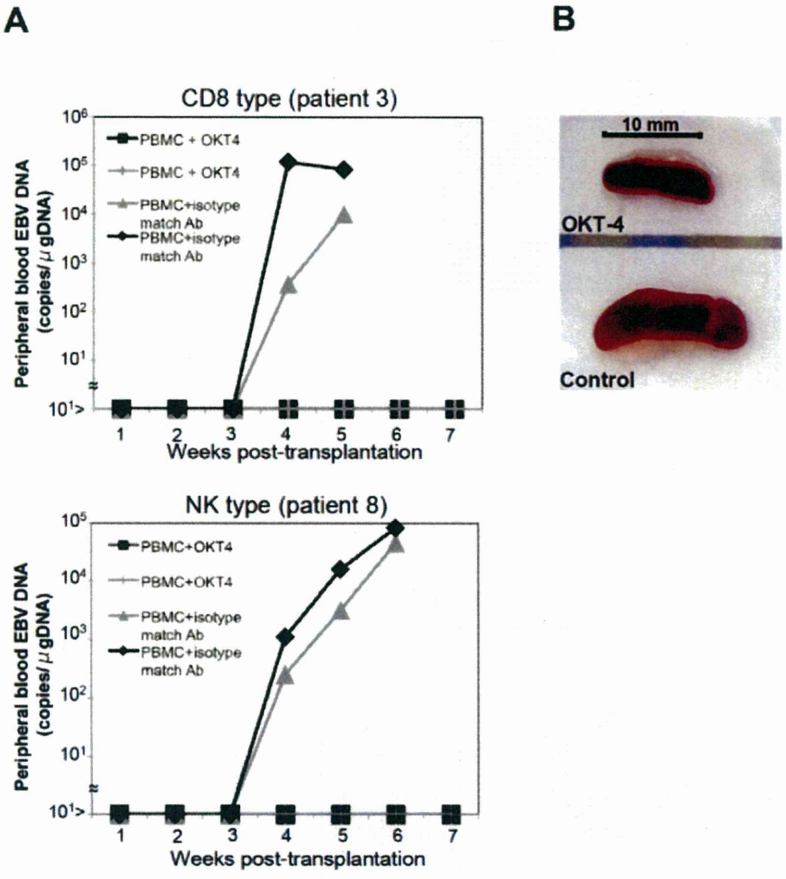

Figure 4. Suppression of the engraftment of EBV-infected T and NK cells by the OKT-4 antibody. PBMC (5×10^6 cells) isolated from the CAEBV patient 3 (CD8 type) or 8 (NK type) were injected intravenously to NOG mice. The OKT-4 antibody (100 μg/mouse) was administered intravenously on the same day of transplantation and the following three consecutive days. As a control, isotype-matched mouse IgG was injected. A. Changes in the peripheral blood EBV DNA level in the recipient mice. Results with the mice transplanted with PBMC of the patient 3 (top) and of the patient 8 (bottom) are shown. B. Photographs of the spleen of an OKT-4-treated mouse (top) and a control mouse (bottom) taken at autopsy.
doi:10.1371/journal.ppat.1002326.g004

II pattern of latent EBV gene expression after engraftment in NOG mice. Similar analyses with NOG mice engrafted with EBV-infected NK cells also showed the latency II type of EBV gene expression (data not shown).

NOG mice engrafted with EBV-infected T or NK cells produce high levels of human cytokines

In patients with CAEBV, high levels of cytokines have been detected in the peripheral blood and are thought to play important roles in the pathogenesis [20,39,40]. To test whether this hypercytokinemia is reproduced in NOG mice, we examined the levels of various human cytokines in the sera of transplanted mice using ELISA kits that can quantify human cytokines specifically. The results are shown in Figure 5B and indicate that the mice transplanted with PBMC of the patient 3 (CD8 type) or the patient 8 (NK type) contained high levels of RANTES, IFN-γ, and IL-8 in their sera.

Engraftment of EBV-infected T and B cells derived from patients with EBV-HLH in NOG mice

To extend the findings obtained from the CAEBV xenograft model to another disease with EBV^+ T/NK lymphoproliferation, we transplanted NOG mice with PBMC isolated from patients with EBV-HLH. Characteristics of the four EBV-HLH patients examined in this study and the results of transplantation with their PBMC are summarized in Table 1. EBV DNA was detected in the peripheral blood three to four weeks post-transplantation and rapidly reached the levels of 1×10^4 to 1×10^6 copies/μg DNA (results of typical experiments are shown in Figure 6A). Similar to the findings in CAEBV, EBV DNA was not detected in the recipient mice, when $CD4^+$ cell fraction was removed from PBMC (Figure 6A). Immunophenotypic analyses on the peripheral blood lymphocytes isolated from EBV-HLH patients and corresponding recipient mice revealed that cells of an identical immunophenotype ($CD3^+CD8^+CD45RO^+CD19^-CD4^-CD45RA^-CD16^-CD56^-$) were present and contained EBV DNA in both the patients and corresponding mice (Figure 6C and data not shown). The EBV DNA load observed in individual lymphocyte subsets in the patient 10 and a mouse that received his PBMC is shown as supporting data (Table S2). General condition of the recipient mice deteriorated consistently more quickly, with the loss of body weight (Figure S1), ruffling of hair, and general inactivity, than those mice engrafted with EBV-infected T or NK cells derived from CAEBV. The mice were sacrificed around four weeks post-transplantation for pathological analyses. Macroscopical observation revealed moderate to severe splenomegaly (Figure 6D) in the

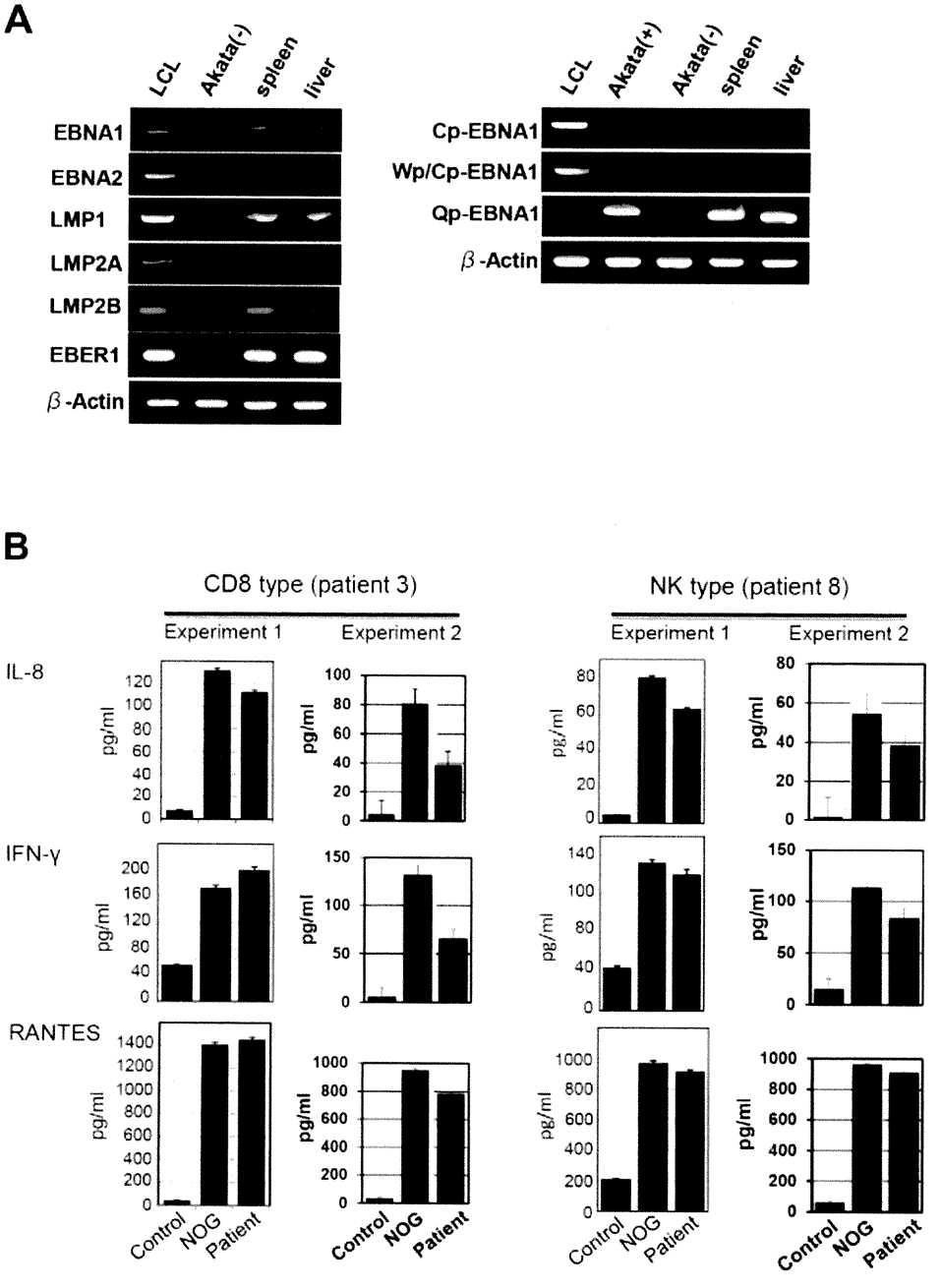

Figure 5. Analyses on the latent EBV gene expression and cytokine production in NOG mice transplanted with PBMC of CAEBV patients. A. EBV gene expression. Total RNA was purified from the spleen and liver of a mouse that received PBMC from the patient 3 (CD8 type) and applied for RT-PCR assay to detect transcripts from the indicated genes. RNA samples from an EBV-transformed B-lymphoblastoid cell line (LCL) and from EBV-negative Akata cell line were used as positive and negative controls, respectively. The primers used in the experiments are shown in Materials and Methods. B. Quantification of plasma levels of human cytokines in patients with CAEBV and corresponding recipient mice. PBMC were isolated from the patients 3 (CD8 type) and 8 (NK type) in two occasions and transplanted to NOG mice. Plasma cytokine levels of the patients were determined when their PBMC were isolated. Plasma cytokine levels of the corresponding recipient mice, prepared on each occasion of PBMC collection, were determined when they were sacrificed. Concentration of human IL-8, IFN-γ, and RANTES were measured by appropriate ELISA kits following the instruction provided by the manufacturer. Plasma samples from healthy adults were used as a control. The bars represent mean values and standard errors from triplicate measurements.
doi:10.1371/journal.ppat.1002326.g005

majority of recipient mice, and slight hepatomegaly in a limited fraction of them. A finding characteristic to these mice were massive hemorrhages in the abdominal and/or thoracic cavities, that were not seen in the mice transplanted with CAEBV-derived PBMC (Figure 6D and data not shown). These hemorrhagic lesions may reflect coagulation abnormalities characteristic to

HLH. Histopathological analyses revealed a number of EBER$^+$ cells in the spleen and the liver (Figure 6E) and quantification of EBV DNA in these tissues revealed 1.4×10^1 to 2.4×10^2 copies/μg of EBV DNA. When the tissues were examined by immunostaining and EBER ISH, the EBER$^+$ cells were shown unexpectedly to be mostly CD45RO$^-$ and CD20$^+$ in all five transplantation experiments with four different patients, indicating that the majority of EBV-infected cells in these tissues are of the B-cell lineage (Figure 6E and data not shown). EBER$^+$ large B cells were seen scattered among numerous reactive small T cells, most of which are CD8$^+$, in the tissues of the spleen, liver, lungs and kidneys. A number of macrophages were also seen in these tissues. Fractionation of mononuclear cells obtained from the liver of a mouse transplanted with PBMC of the EBV-HLH patient 10, followed by real-time PCR, detected EBV DNA (1.4×10^1 copies/μg DNA) only in the CD19$^+$ B-cell fraction. In addition, an EBV-infected B lymphoblastoid cell line, but not an EBV-positive T cell line, could be established from this liver. Thus the presence of EBV in B cells were demonstrated by three independent methods in the tissues of EBV-HLH mice. Enzyme-linked immunosorbent assay revealed extremely high levels of human cytokines, including IL-8, IFN-γ, and RANTES, in the sera of both the original patients and the recipient mice (Figure 6B). The levels of IL-8 and IFN-γ were much higher than those observed in the peripheral blood of patients with CAEBV and mice that received their PBMC. Thus, NOG mice transplanted with EBV-HLH-derived PBMC are distinct from those transplanted with CAEBV-derived PBMC in the aggressive time course of the disease, internal hemorrhagic lesions, extremely high levels of IL-8 and IFN-γ in the peripheral blood, and the presence of EBV-infected B cells in lymphoid tissues.

Discussion

The mouse xenograft models of CAEBV and EBV-HLH developed here represent the first recapitulation of EBV-associated T/NK lymphoproliferation in experimental animals. Previously, Hayashi and others inoculated rabbits with Herpesvirus papio and succeeded in the generation of T-cell lymphoproliferative disorder with pathological findings suggestive of EBV-HLH [41]. This model, however, is based on an EBV-related virus and not EBV itself, and therefore may contain features irrelevant to the original human disease. Although the CAEBV and EBV-HLH models described here exhibited some common features, including the abundant presence of EBV-infected T or NK cells in the peripheral blood, there were some critical differences between the two models, probably reflecting the divergence of the pathophysiology of the original diseases. First of all, in the EBV-HLH model mouse, EBV was detected mainly in B cells in the spleen and the liver, while it was found mainly in T cells in the peripheral blood. This makes an obvious contrast with the CAEBV model mouse, where EBV was detected in T or NK cells in both the peripheral blood and lymphoid tissues. We do not have an explanation for the apparent discrepancy in the host cell type of EBV infection between the peripheral blood and lymphoid tissues of the EBV-HLH model. It should be, however, noted that histopathology of EBV-HLH tissues has not been fully investigated and therefore it is still possible that significant number of EBV-infected B cells are present in the lymphoid tissues of EBV-HLH patients. Other differences between the two models include much higher plasma levels of IL-8 and IFN-γ more aggressive and fatal outcome, and internal hemorrhagic lesions in EBV-HLH model mice, probably reflecting the differences in the pathophysiology of the original diseases.

EBV-positive B-cell proliferation was not seen in CAEBV model mice even in long-term observation beyond twelve weeks. This seems puzzling since low but significant amount of EBV DNA was found also in B19$^+$ B-cell fraction in most patients with CAEBV. It should be noted that EBV-infected T or NK cell lines could be established relatively easily from patients with CAEBV by adding recombinant IL-2 in the medium. In contrast, establishment of EBV-infected B LCLs from these patients has been extremely difficult. In fact, we could establish B-LCLs from a few patients with CAEBV only when their PBMC were cultured on feeder cells expressing CD40 ligand. Therefore, we speculate that in the particular context of CAEBV, both in the patient and the model mouse, proliferation of EBV-infected B cells are somehow inhibited by an unknown mechanism.

Analysis on the conditions of engraftment of EBV-infected T/NK cells using these new xenograft models revealed that EBV-infected T and NK cells of the CD8$^+$ T, TCRγδT and CD56$^+$ NK lineages and cell lines derived from them require CD4$^+$ T cells for their engraftment in NOG mice. Only those EBV-infected cells and cell lines of the CD4$^+$ T lineage could engraft in NOG mice on their own. These findings suggest that some factor(s) provided by CD4$^+$ cells are essential for engraftment. Soluble factors produced by CD4$^+$ T cells may be responsible for this function and we are currently examining cytokines, including IL-2, for their ability to support the engraftment of EBV-infected T and NK cells. It is also possible that cell to cell contact involving CD4$^+$ cells is critical for engraftment. This dependence on CD4$^+$ cells represents an interesting consistency with the previous finding that engraftment of EBV-transformed B lymphoblastoid cells in *scid* mice required the presence of CD4$^+$ cells [42,43]. It has been speculated that T cells activated by an EBV-induced superantigen may be involved in the engraftment of EBV-infected B lymphoblastoid cells in *scid* mice [44]. Although a similar superantigen-mediated mechanism might also be assumed in T- and NK-cell lymphoproliferation in NOG mice, the data of TCR repertoire analyses (Figure 1C and data not shown) show no indication for clonal expansion of Vβ13 T cells that are known to be specifically activated by the EBV-induced superantigen HERV-K18. It seems therefore unlikely that this superantigen is involved in the CD4$^+$ T cell-dependent engraftment of EBV-infected T and NK cells. We expect CD4$^+$ T cells and/or molecules produced by them may be an excellent target in novel therapeutic strategies for the treatment of CAEBV and EBV-HLH. In fact, administration of the OKT-4 antibody that depletes CD4$^+$ cells in vivo efficiently prevented the engraftment of EBV-infected T cells. As a next step, we plan to test the effect of post-engraftment administration of OKT-4.

The dependence of EBV-infected T and NK cells on CD4$^+$ T cells for their engraftment in NOG mice suggests the possibility that these cells are not capable of autonomous proliferation. Consistent with this notion, EBV-infected T and NK cell lines, including that of the CD4$^+$ lineage, are dependent on IL-2 for their in vitro growth and do not engraft in either nude mice or *scid* mice when transplanted either s.c. or i.v (Shimizu, N., unpublished results). Clinically, CAEBV is a disease of chronic time course and patients carrying monoclonal EBV-infected T or NK cell population may live for many years without progression of the disease [15]. Overt malignant T or NK lymphoma usually develops only after a long course of the disease. Taking all these findings in consideration, we suppose that EBV-infected cells are not truly malignant at least in the early phase of the disease, even when they appear monoclonal. Because infection of EBV in T or NK cells is not unique to CAEBV and has been recognized also in infectious mononucleosis [45,46], the critical deficiency in